tion (Manassas, VA). These cells were maintained in RPMI1640 media supplemented with 2 mM glutamine, 1% nonessential amino acids, 100 U/ml streptomycin/penicillin and 10% fetal calf serum (FCS).

Western blot analysis was performed using protein extracts obtained from 4 strains of PrEC, LNCaP, DU145 and PC-3 cells. Briefly, cells were rinsed twice with ice-cold phosphate-buffered saline (PBS) and lysed in 180 μl Nonidet P-40 lysis buffer (50 mM Tris-HCl [pH 7.4], 150 mM NaCl, 10 mM NaF, 5 mM EDTA, 5 mM EGTA, 2 mM sodium vanadate, 0.5% sodium deoxycholate, 1 mM dithiothreitol [DTT], 1 mM phenylmethylsulfonylfluoride [PMSF], 2 μg/ml aprotinin and 0.1% Nonidet P-40), and the lysates were cleared by centrifugation at 15,000*g* for 15 min at 4°C. Total protein lysate (20 μg) of each cell line was fractionated on sodium dodecyl sulfate (SDS)-12.5% polyacrylamide gels, and electrophoretically transferred onto polyvinylidene difluoride (PVDF) membranes (Immobilon, Millipore Co., Bedford, MA). The membranes were blocked in Tris-buffered saline (TBS) with 5% skim milk for 30 min, then incubated with 5 ml each of 1:1,000 diluted purified anti-EBAG9 antibody at room temperature for 3 hr. Each membrane was washed in TBS with 0.1% Tween 20 and incubated with 1:5,000 diluted horseradish peroxidase-conjugated donkey anti-rabbit immunoglobulin (Ig)G (Amersham Pharmacia Biothech, Arlington Heights, IL) at room temperature for 1 hr. Bands were visualized with the chemiluminescence-based ECL plus detection system (Amersham Pharmacia Biotech). The membranes were exposed to X-ray film. All experiments were performed a minimum of 3 times.

Patients and tissue sections

Formalin-fixed paraffin-embedded sections were obtained from 21 benign prostatic hyperplasia and 81 clinically localized prostatic cancer specimens surgically resected at Tokyo University hospital. The age of the patients ranged from 51–77 years (mean 62.7 ± 5.9), and pretreatment serum prostate-specific antigen (PSA) level of 81 cancer patients ranged from 4.1–131.0 ng/ml (mean 29.1 ± 30.1). The pathologic stages of the cancers included B (n = 23), C (n = 45) and D_1 (n = 13). The cancerous lesions consisted of tumors with the Gleason scores 4 (n = 15), 5 (n = 8), 6 (n = 10), 7 (n = 14), 8 (n = 14), 9 (n = 17) and 10 (n = 3). High-grade prostatic intraepithelial neoplasia (HGPIN) was identified in 65 cancer specimens (80%). One hundred forty-six foci of HGPIN were submitted for study. Of 13 pathologic stage-D_1 tumors, 10 tissue sections of lymph node metastasis were also included for our study.

No patients with the cancer underwent neoadjuvant anti-androgen therapy. Forty-nine cancer patients (60%) were treated with surgery alone, whereas the remaining patients received anti-androgen therapy after radical prostatectomy. Patients were followed postoperatively on a monthly basis until social urinary continence (one or no pad used/day) was obtained and then at 3-month intervals to 5 years, and yearly thereafter. Mean patient follow-up period was 43.0 ± 19.1 months (range 2–85 months). PSA-failure was used as a prognostic endpoint for our study and defined by a serum PSA concentration ≥ 0.4 ng/ml rising over a 3-month period. During the follow-up period, 45 patients (56%) were alive with no evidence of the relapse, and 36 (44%) were alive with PSA-failure. No patients died of prostatic cancer or other diseases during the study period.

Immunohistochemic analysis

Immunohistochemic analysis was performed employing the streptavidin-biotin amplification method using an EnVision+ (DAKO, Carpinteria, CA). Tissue-sections (6-μm thick) were deparaffinized, rehydrated through graded ethanol and rinsed in PBS. For antigen retrieval, the sections were heated in an autoclave at 120°C for 5 min in citric acid buffer (2 mM citric acid and 9 mM trisodium citrate dehydrate, pH6.0) for the immunostaining of EBAG9, ERα, and ERβ or incubated with 0.05% protease in 50mM Tris-HCl buffer, pH7.6 for 10 min for CD3. After blocking endogenous peroxidase with 0.3% H_2O_2, the sections were incubated in 10% bovine serum for 30 min. The primary antibody for EBAG9 (1:80 dilution), ERα (1:100), ERβ (1:80), or CD3 (1:200) was applied and incubated at 4°C over night. After rinsing in PBS, sections were incubated with EnVision+; anti-rabbit (for EBAG9, ERβ, and CD3) or anti-mouse (for ERα) for 1 hr at room temperature according to the manufacturer's instructions. The antigen-antibody complex was visualized with 3,3′-diaminobenzidine (DAB) solution (1 mM DAB, 50mM Tris-HCl buffer [pH 7.6] and 0.006% H_2O_2). Sections of EBAG9 immunodetection were then counterstained in hematoxylin. Negative controls were treated in the same way, but the primary antibodies were replaced by normal rabbit or mouse IgG.

For immunohistochemic assessment, 3 investigators (ST, TU and TF) evaluated the tissue sections independently. Intense immunostaining in the cytoplasm (for EBAG9) and cell nucleus (for ERα and ERβ) was defined as positive. The sections with <5% reactive cells were considered negative (–): 5% to 25%, 25% to 50% and >50% reactive cells were defined as 1+, 2+ and 3+, respectively. The number of $CD3^+$ cells on high-power fields (×400) was counted to determine the infiltration of T lymphocytes. For each specimen, 6 fields were selected at random in the invasive margin of the cancer. Cases with discordant results among the investigators were reevaluated.

Statistical analysis

Correlation between EBAG9 immunoreactivity and clinicopathologic characteristics (age, pretreatment serum PSA level, pathologic stage, Gleason score and site of specimen and immunoreactivity of ERα and ERβ) were evaluated using the t-test or Fisher's exact probability test. PSA failure-free survival curves were obtained by the Kaplan-Meier method and verified by the Log-rank (Mantel-Cox) test. The Cox's proportional hazards regression model was used to calculate risk ratios for univariate analyses of factors potentially related to PSA failure and to determine whether those factors are independent prognostic predictors in the presence of other clinicopathological markers. For all statistical analyses, p-values less than 0.05 were regarded as significant.

RESULTS

Western blot analysis

Using the polyclonal anti-EBAG9 antibody, a 32-kDa band, which corresponded to the molecular weight of EBAG9, was detected in both normal PrECs and prostate cancer cells (LNCaP, DU145 and PC-3). In the prostate cancer cells (especially in LNCaP), the bands were detected at a higher intensity compared to normal PrECs (Fig. 1).

FIGURE 1 – Western blot analysis of EBAG9. The cell extracts from PrECs and prostate cancer cells (LNCaP, DU145 and PC-3) were resolved by SDS-PAGE and transferred to PVDF membrane. Blot was probed with the EBAG9-specific polyclonal antibody (1:1,000), and a 32-kDa band was detected in both normal PrECs and prostate cancer cells (LNCaP, DU145 and PC-3). In the prostate cancer cells (especially in LNCaP), the bands were detected at a higher intensity compared to normal PrECs.

Immunohistochemistry

Immunoreactivity of EBAG9 was weakly detected at the luminal cells of benign epithelium (data not shown). However, intense and diffuse immunostaining of EBAG9 in the cytoplasm was not identified in the benign epithelial compartment. In contrast, strong EBAG9 immunoreactivity diffusely existed in the cytoplasm of cancer cells (Fig. 2). Of 81 prostatic cancer cases, EBAG9 immunoreactivity was 1+ in 7 (9%), 2+ in 15 (18%) and 3+ in 22 (27%) specimens. When 1+ or more were defined as positive, EBAG9 expression was identified in 44 (54%) cancer cases. As for 146 HGPIN lesions, EBAG9 expression (≧1+) was observed in only 18 foci (12%).

As previously reported[19,22], strong immunostaining of ERα was identified in stromal compartment of both the benign and malignant tissue. In contrast, ERα was variably expressed in epithelial compartment. Only focal ERα expression, which was generally restricted to basal cells was found in a minority of the benign epithelium. Positive ERα immunoreactivity (≧1+) was detected in 10 (12%) cancerous specimens. ERβ was preferentially expressed in epithelial compartment of both the benign and malignant prostate. All 21 benign hyperplasia specimens showed strong staining (3+) for ERβ in both the basal cells and luminal secretory epithelium. Of 81 cancer cases, ERβ immunoreactivity was negative in 24 (30%), 1+ in 27 (33%), 2+ in 21 (26%) and 3+ in 9 (11%) specimens. ERβ expression was inversely correlated with Gleason grade ($p = 0.0068$). $CD3^+$ cells were found mainly in the invasive margin of the cancer as well as in the stroma, and the distribution pattern was similar to that of leukocytes by conventional H&E stain.

Clinicopathologic correlates of EBAG9 immunostaining in prostatic cancers

Potential correlation between EBAG9 immunoreactivity and clinicopathologic characteristics (age, pretreatment serum PSA level, pathologic stage, Gleason score and site of specimen, immunoreactivity of ERα and ERβ, and infiltration of $CD3^+$ cells) were evaluated (Table I). Pathologic stage-D_1 tumor exhibited positive EBAG9 immunoreactivity more frequently than stage B and C diseases ($p = 0.0305$). Strong correlation was found between EBAG9 expression status and Gleason score (GS) ($p < 0.0001$). Of 48 higher GS (≥ 7) tumors, 40 (83%) were positive for EBAG9 expression, while only 4 (12%) of 33 lower GS (≤ 6) tumors were EBAG9-positive (Fig. 2*a* and *b*). In order to determine correlation of EBAG9 expression with the tumor progression, we investigated EBAG9 immunoreactivity in sites of capsular penetration ($n = 28$) and lymph node metastasis ($n = 10$). EBAG9 was more frequently expressed at sites of capsular penetration, compared to intracapsular primary lesions ($p = 0.0264$). Furthermore, all 10 lesions of lymph node metastasis (100%) were EBAG9-positive, while 44 of 81 (54%) primary sites were positive ($p = 0.0048$, Fig. 2*c*). No significant correlation was found between EBAG9 expression and immunoreactivity of ERα and ERβ ($p = 0.7480$ and $p = 0.8075$, respectively). A trend that $CD3^+$ cells more infiltrate into the invasive margin of the EBAG9-negative tumors than EBAG9-positive tumors was observed. However, it did not reach statistical significance ($p = 0.0637$).

Kaplan-Meier analysis of PSA failure-free survival of prostatic cancer cases with positive and negative EBAG9 immunoreactivity is shown in Figure 3. Twenty-six of the 44 (59%) EBAG9-positive cases had PSA failure during the follow-up. Patients with EBAG9-positive prostatic cancer had significantly worse PSA failure-free survival than those with EBAG9-negative tumor ($p = 0.0059$, log-rank test). The results of Cox proportional hazard analyses of various prognostic factors in prostatic cancer patients are shown in Table II. In the univariate analysis, EBAG9 expression was significantly ($p = 0.0087$) related to PSA failure-free survival as well as the Gleason score ($p = 0.0086$) and pathologic stage ($p = 0.0082$). Furthermore, patients with tumors negative for ERβ immunoreactivity had significantly higher risk of PSA failure ($p = 0.0346$) as we reported previously[19]. In multivariate analysis, however, EBAG9 expression was not an independent predictor (risk ratio; 2.118, $p = 0.1674$), and pathological stage was the only independent marker of other clinicopathological parameters for PSA failure-free survival (risk ratio; 2.481, $p = 0.0279$).

DISCUSSION

In our present study, we first demonstrated EBAG9 expression in human normal and malignant prostatic epithelial cells by West-

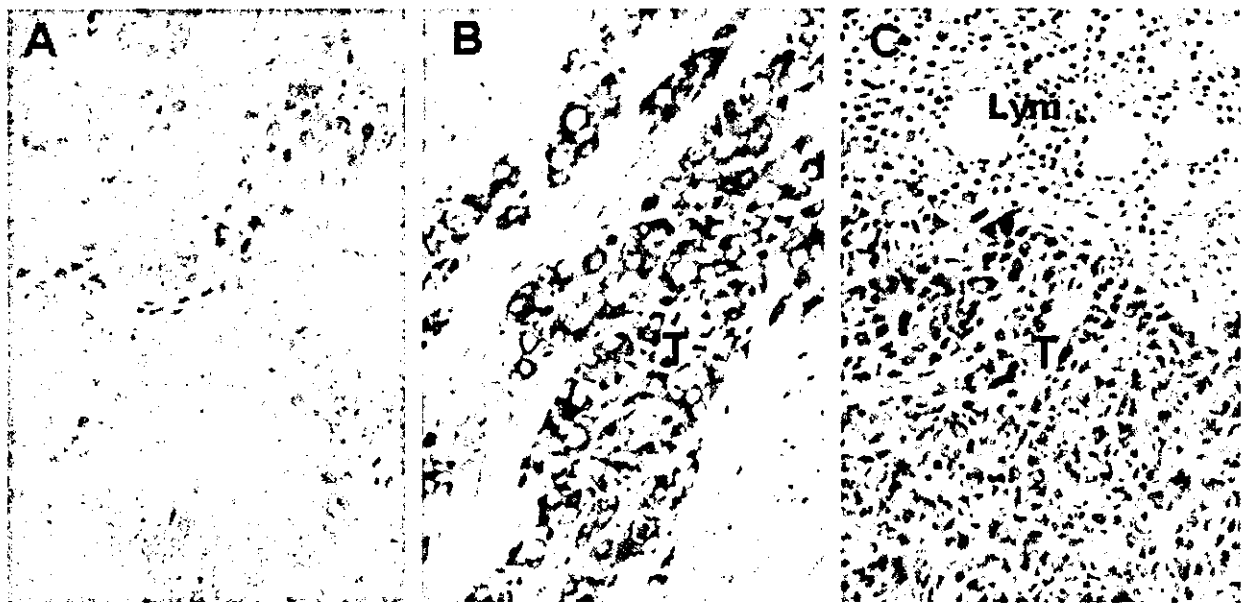

FIGURE 2 – Representative photographs of immunohistochemic staining of EBAG9 in human prostatic cancer. Although weak immunoreactivity of EBAG9 is localized in the perinuclear region of the cytoplasm, no significant expression of EBAG9 was identified in Gleason score 4 cancer (–). *(a)* Strong and diffuse immunostaining in the cytoplasm is observed in > 50% of a Gleason score 9 cancerous lesion (T) (3+). *(b)* EBAG9 is highly expressed in an entire metastatic lesion (T) of pelvic lymph node (Lym) (3+). *(c)* Original magnification; ×400.

TABLE 1 - CORRELATION BETWEEN EBAG9 EXPRESSION AND CLINICOPATHOLOGICAL CHARACTERISTICS IN HUMAN PROSTATIC CANCER (N = 81)

Clinicopathological characteristics	EBAG9 expression[1]		
	Negative	Positive	p^2
Age (yrs)	61.8 ± 6.5	63.5 ± 5.2	0.1742
Pretreatment serum PSA level (ng/ml)	24.8 ± 24.9	32.7 ± 33.8	0.2414
Pathological stage			
B, C	35	33	0.0305
DI	2	11	
Gleason score			
≦ 6	29	4	<0.0001
≧ 7	8	40	
Site of specimen[3]			
Intracapsular (primary)	37	44	
Capsular penetration	6	22	0.0264
Lymph node metastasis	0	10	0.0048
ERα[1]			
Negative	33	38	0.7480
Positive	4	6	
ERβ[1]			
Negative	10	14	0.8075
Positive	27	30	
Infiltration of CD3-positive cells	77.9 ± 21.9	69.5 ± 18.2	0.0637

[1]Degree of the immunoreactivity: 1+, 2+, and 3+ was defined as positive;–[2]Correlation between Expression of EBAG9 protein and clinicopathological characteristics was evaluated using the t-test or Fisher's exact probability test.–[3]EBAG9 expression status in sites of capsular penetration (n = 28) and lymph node metastasis (n = 10) was compared with that in intracapsular primary lesions (n = 81).

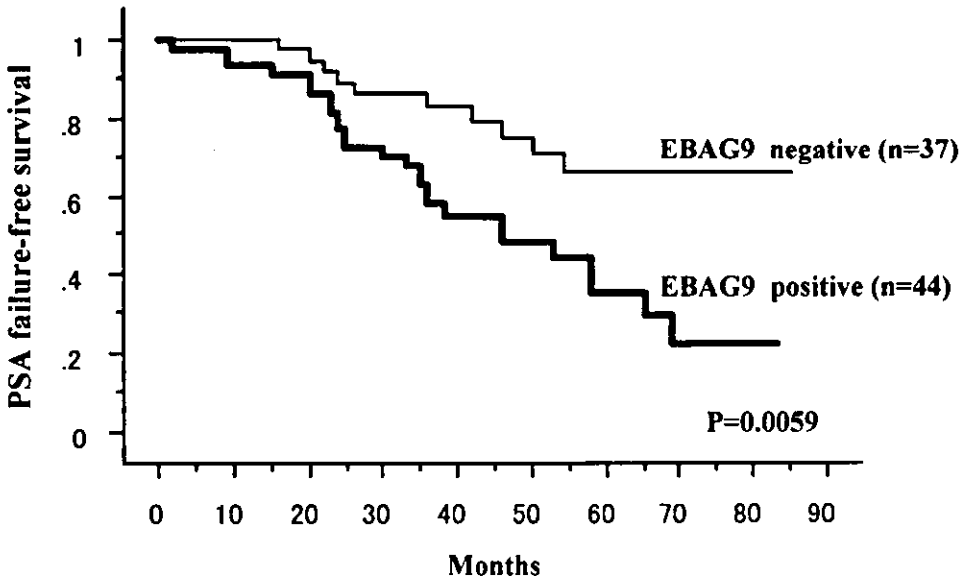

FIGURE 3 – Kaplan-Meier analysis of PSA failure-free survival in patients treated for clinically localized prostatic cancer stratified for EBAG9 expression. p = 0.0059 by the log-rank test.

ern blot and immunohistochemic analyses. EBAG9 immunoreactivity in the normal or hyperplastic prostatic epithelium was low and restricted to the luminal cells, but not basal cells, while intense and diffuse EBAG9 expression was found in the cytoplasm of the cancer cells. EBAG9/RCAS1 has been also reported to exist in other normal organs, including bronchi, gastric mucosa, mammary glands and uterine endometrial glands.[9,12,14,23]. Kubokawa *et al.*[12] found that EBAG9/RCAS1 is localized in the perinuclear region of the normal gastric mucosal cells, while in most of gastric cancers, it was detected diffusely in the cytoplasm and cell membranes of the tumor cells. Although the physiologic roles of EBAG9/RCAS1 in normal tissue are unknown, alterations of its intracellular distribution may be associated with carcinogenesis and cancer progression.

Increased EBAG9/RCAS1 expression has been recently found in various human carcinomas, including uterine, ovarian, lung, hepatic, skin, gastric and breast cancers.[3–5,8–14] EBAG9/RCAS1 expression is also associated with aggressive phenotypes of tumors, such as poor cell differentiation and advanced stages.[5,8,9,11–13] Furthermore, EBAG9/RCAS1 expression has been reported to correlate with poor prognosis in patients with uterine cervical adenocarcinoma and non small cell lung cancer.[8,9,11] In our present study, increased EBAG9 immunoreactivity significantly correlated with advanced pathologic stages and high Gleason score of prostatic cancer. Furthermore, positive EBAG9 expression significantly correlated with poor PSA failure-free survival. On the other hand, EBAG9 was expressed in only 12% of HGPIN lesions, which was considered to be a precursor of high-

TABLE 2 – COX PROPORTIONAL HAZARDS ANALYSIS OF CLINICOPATHOLOGICAL DATA AND EBAG9 EXPRESSION IN 81 PATIENTS WITH PROSTATIC CANCER

Variable	Unfavorable/Favorable[1]	Risk ratio	*p*
Age (yrs)	≤65/>65	1.222	0.5809
Pretreatment PSA level (ng/ml)	>20/≤20	1.735	0.1047
Pathological stage	D1/B, C	2.724	0.0082
Gleason score	≥7/≤6	2.877	0.0086
ERα	Positive/negative	1.836	0.1771
ERβ	Negative/positive	2.090	0.0346
EBAG9	Positive/negative	2.660	0.0087

[1]Unfavorable *vs.* favorable characteristics.

grade prostatic carcinoma. These findings suggest that EBAG9/RCAS1 increases its expression in the development of various types of human cancers, and may play a significant role to obtain their aggressive phenotypes. In the present study, however, the multivariate analysis of prognostic markers could not demonstrate that EBAG9 expression is an independent predictor for PSA failure. Further studies are warranted to well define the prognostic and therapeutic significance of EBAG9/RCAS1 in patients with prostatic cancer.

EBAG9/RCAS1 acts as a ligand for a putative receptor present on human T, B, NK and other hematopoietic cells.[6,24] The receptor expression was enhanced by activation of the lymphocytes. EBAG9/RCAS1 induces cell arrest and apoptosis in activated $CD3^+$ T lymphocytes, consistent with the idea that EBAG9/RCAS1 might be involved in tumor immune escape.[6,7] Iwasaki *et al.*[9] evaluated the apoptotic index (AI) of tumor-infiltrating lymphocytes (TILs) in EBAG9/RCAS1-expressing lung cancers, and found that AI values of high EBAG9/RCAS1-expressing cases was significantly higher than those of low expressing cases. A similar finding was observed in human breast cancer, suggesting that EBAG9/RCAS1 may inhibit the intratumoral infiltration of T lymphocytes.[14] It has been reported that the density of TILs in prostatic cancer is independent of tumor differentiation, and absent or weak TILs were signs of a high risk of tumor progression and of a fatal disease.[25] In the present study, a trend that $CD3^+$ cells less infiltrate into the margin of the EBAG9-positive tumors than EBAG9-negative tumors was observed ($p = 0.0637$). Furthermore, the following findings may partly support a hypothesis that EBAG9/RCAS1 suppresses immune attack of activated T lymphocytes in prostatic cancer, as well. In immunohistochemic analysis, EBAG9/RCAS1 was more frequently detected at sites of capsular penetration compared to intracapsular primary lesions. Furthermore, all 10 lesions of lymph node metastasis evaluated were immunopositive for EBAG9/RCAS1. These findings suggest that prostatic cancers expressing EBAG9/RCAS1 may evade immune surveillance and subsequently progress to metastatic diseases.[6,7]

EBAG9 has been identified as an estrogen-responsive gene from a cDNA library of MCF-7 human breast cancer cells, which express ERα and low level of ERβ[1,26] Transfection analyses have demonstrated that the nucleotide sequence between −86 to −36 contains an ERE in the 5′-promoter region of the EBAG9 gene.[27] mRNA levels of EBAG9 in MCF-7 cells are significantly increased within 6 hr of estrogen treatment.[22] The present study and recent investigations have revealed that ERα and ERβ are preferentially expressed in the stromal and epithelial compartment of normal prostate, respectively.[16–19] In contrast, prostatic cancer cells more variably express both ERα and ERβ.[16–19,22,28,29] Therefore, EBAG9 expression in prostatic cancer may be regulated via ERα and/or ERβ signaling pathways, subsequently playing a role in carcinogenesis and cancer development. The present study, however, did not show significant correlation between EBAG9 and ERs expression. Furthermore, a finding of frequent loss of ERβ immunoreactivity in high Gleason-grade cancers, which often express EBAG9, raises a question; "What regulates EBAG9 expression in these cancers?" Promoter analysis of EBAG9 has demonstrated that 5′-flanking region of EBAG9 contains not only ERE, but also other putative binding sites for transcription factors, such as 5 GC-boxes (GGGCGG) and 5 E-boxes (CANNTG).[27] These findings suggest that other mechanisms independent of ER signaling pathways may also contribute to regulation of EBAG9 expression in prostatic cancer cells.

In conclusion, we demonstrated EBAG9/RCAS1 expression in human normal and malignant prostate. Increased EBAG9/RCAS1 expression in prostate cancer was associated with the aggressive phenotypes and poor prognosis. These results suggest that EBAG9/RCAS1 may play a significant role in prostatic cancer progression via an immune escape system. Immunohistochemic evaluation of EBAG9/RCAS1 expression can be an adjunctive prognostic indicator for patients with prostatic cancer.

REFERENCES

1. Watanabe T, Inoue S, Hiroi H, Orimo A, Kawashima H, Muramatsu M. Isolation of estrogen-responsive genes with a CpG island library. Mol Cell Biol 1998;18:442–9.
2. Tsuchiya F, Ikeda K, Tsutsumi O, Hiroi H, Momoeda M, Taketani Y, Muramatsu M, Inoue S. Molecular cloning and characterization of mouse EBAG9, homolog of a human cancer associated surface antigen: expression and regulation by estrogen. Biochem Biophys Res Commun 2001;284:2–10.
3. Sonoda K, Nakashima M, Saito T, Amada S, Kamura T, Nakano H, Watanabe T. Establishment of a new human uterine cervical adenocarcinoma cell line, SiSo, and its reactivity to anti-cancer reagents. Int J Oncol 1995;6:1099–104.
4. Sonoda K, Nakashima M, Kaku T, Kamura T, Nakano H, Watanabe T. A novel tumor-associated antigen expressed in human uterine and ovarian carcinomas. Cancer (Phila) 1996;77:1501–9.
5. Sonoda K, Kaku T, Kamura T, Nakashima M, Watanabe T, Nakano H. Tumor-associated antigen 22-1-1 expression in the uterine cervical squamous neoplasias. Clin Cancer Res 1998;4:1517–20.
6. Nakashima M, Sonoda K, Watanabe T. Inhibition of cell growth and induction of apoptotic cell death by the human tumor-associated antigen RCAS1. Nature Med 1999;5:938–42.
7. Villunger A, Strasser A. The great escape: is immune evasion required for tumor progression? Nature Med 1999;5:874–5.
8. Kaku T, Sonoda K, Kamura T, Hirakawa T, Sakai K, Ameda S, Ogawa S, Kobayashi H, Nakashima M, Watanabe T, Nakano H. Prognostic significance of tumor-associated antigen 22-1-1 expression in adenocarcinoma of the uterine cervix. Clin Cancer Res 1999;5:1449–53.
9. Iwasaki T, Nakashima M, Watanabe T, Yamamoto S, Inoue Y, Yamanaka H, Matsumura A, Iiuchi K, Mori T, Okada M. Expression and prognostic significance in lung cancer of human tumor-associated antigen RCAS1. Int J Cancer 2000;89:488–93.
10. Noguchi K, Enjoji M, Nakamuta M, Nakashima M, Nishi H, Choi I, Taguchi K, Kotoh K, Shimada M, Sugimachi K, Tsuneyoshi M, Nawata H, Watanabe T. Expression a tumor-associated antigen RCAS1 in hepatocellular carcinoma. Cancer Lett 2001;168:197–202.
11. Izumi M, Nakanishi Y, Yoshino I, Nakashima M, Watanabe T, Hara N. Expression of tumor-associated antigen RCAS1 correlates significantly with poor prognosis in nonsmall cell lung carcinoma. Cancer 2001;92:446–51.
12. Kubokawa M, Nakashima M, Yao T, Ito KI, Harada N, Watanabe T.

Aberrant intracellular localization of RCAS1 is associated with tumor progression of gastric cancer. Int J Oncol 2001;19:695–700.
13. Takahashi H, Iizuka H, Nakashima M, Wada T, Asano K, Ishida-Yamamoto A, Watanabe T. RCAS1 antigen is highly expressed in extra mammary Paget's disease and in advanced stage squamous cell carcinoma of the skin. J Dermatol Sci 2001;26:140–4.
14. Suzuki T, Inoue S, Kawabata W, Akahira J, Moriya T, Tsuchiya F, Ogawa S, Muramatsu M, Sasano H. EBAG9/RCAS1 in human breast carcinoma: a possible factor in endocrine-immune interactions. Br J Cancer 2001;85:1731–7.
15. Kuiper CG, Enmark E, Pelto-Huikko M, Nilson S, Gustafsson JA. Cloning of a novel estrogen receptor expressed in rat prostate and ovary. Proc Natl Acad Sci USA 1996;93:5925–30.
16. Lau KM, LaSpina M, Long J, Ho SM. Expression of estrogen receptor (ER)-α and ER-β in normal and malignant prostate epithelial cells: regulation by methylation and involvement in growth regulation. Cancer Res 2000;60:3175–82.
17. Leav I, Lau KM, Adams JY, McNeal JE, Taplin M-E, Wang J, Singh H, Ho Shuk-Mei. Comparative studies of the estrogen receptors β and α and the androgen receptor in normal human prostate glands, dysplasia, and in primary and metastatic carcinoma. Am J Pathol 2001; 159:79–92.
18. Pasquali D, Staibono S, Prezioso D, Franco R, Esposito D, Notaro A, De Rosa Gaetano, Bellastella A, Antonio N. Estrogen receptor β expression in human prostate tissue. Mol Cell Endocrinol 2001;178: 47–50.
19. Fujimura T, Takahashi S, Urano T, Ogawa S, Ouchi Y, Kitamura T, Muramatsu M, Inoue S. Differential expression of estrogen receptor β (ERβ) and its C-terminal truncated splice variant ERβcx as prognostic predictors in human prostatic cancer. Biochem Biophys Res Commun 2001;289:692–9.
20. Ogawa S, Inoue S, Watanabe T, Hiroi H, Orimo A, Hosoi T, Ouchi Y, Muramatsu M. Molecular cloning and characterization of human estrogen receptor beta-cx: A potential inhibitor of estrogen action in human. Nucleic Acids Res 1998;26:3505–12.
21. Hiroi H, Inoue S, Watanabe T, Goto W, Orimo A, Momoeda M, Tsutsumi O, Taketani Y, Muramastu M. Differential immunolocalization of estrogen receptor α and β in rat ovary and uterus. J Mol Endocrinol 1999;22:37–44.
22. Harvath LG, Henshall SM, Lee CS, Head DR, Quinn DI, Makela S, Delprado W, Golovsky D, Brenner PC, O'Neill G, Kooner R, Stricker PD, et al. Frequent loss of estrogen receptor-β expression in prostate cancer. Cancer Res 2001;61:5331–5.
23. Sonoda K, Kaku T, Hirakawa T, Kobayashi H, Amada S, Sakai K, Nakashima M, Watanabe T, Nakano H. The clinical significance of tumor-associated antigen RCAS1 expression in the normal, hyperplastic, and malignant uterine endometrium. Gynecol Oncol 2000;79: 424–9.
24. Matsushima T, Nakashima M, Oshima K, Abe Y, Nishimura J, Nawata H, Watanabe T, Muta K. Receptor binding cancer antigen expressed on SiSo cells, novel regulator of apoptosis of erythroid progenitor cells. Blood 2001;98:313–21.
25. Vesalainen S, Lipponen P, Talja M, Syrjanen K. Histological grade, perineural infiltration, tumor-infiltrating lymphocytes and apoptosis as determinants of long-term prognosis in prostatic adenocarcinoma. Eur J Cancer 1994;30A:1797–1803.
26. Vladusic EA, Hornby AE, Guerra-Vladusic FK, Lakins J, Lupu R. Expression and regulation of estrogen receptor beta in human breast tumors and cell lines. Oncol Rep 2000;7:157–67.
27. Ikeda K, Sato M, Tsutsumi O, Tsuchiya F, Tsuneizumi M, Emi M, Imoto I, Inazawa J, Muramatsu M, Inoue S. Promoter analysis and chromosomal mapping of human EBAG9 gene. Biochem. Biophys Res Commun 2000;273:654–60.
28. Royuela M, de Miguel MP, Bethencourt FR, Sanchez-Chapado M, Frile B, Arenas MI, Paniagua R. Estrogen receptor α and β in the normal, hyperplastic and carcinomous human prostate. J Endocrinol 2001;168:447–54.
29. Bonkhoff H, Fixemer T, Hunsicker I, Remberger K. Estrogen receptor expression in prostate cancer and premalignant prostatic lesions. Am J Pathol 1999;155:641–7.

0013-7227/03/$15.00/0
Printed in U.S.A.

The Journal of Clinical Endocrinology & Metabolism 88(3):1333–1340

doi: 10.1210/jc.2002-021015

Zone-Dependent Expression of Estrogen Receptors α and β in Human Benign Prostatic Hyperplasia

TOSHIFUMI TSURUSAKI, DAIYU AOKI, HIROSHI KANETAKE, SATOSHI INOUE, MASAMI MURAMATSU, YOSHITAKA HISHIKAWA, AND TAKEHIKO KOJI

Department of Urology (T.T.), The Japanese Red Cross Nagasaki Atomic Bomb Hospital, Nagasaki 852-8511; Department of Urology (D.A., H.K.), Nagasaki University School of Medicine, Nagasaki 852-8501; Department of Biochemistry (S.I., M.M.), Saitama Medical School, Saitama 350-0495; and Department of Histology and Cell Biology (T.T., Y.H., T.K.), Nagasaki University School of Medicine, Nagasaki 852-8523, Japan

Estrogen, which acts through estrogen receptors (ERs) α and β, has been implicated in the pathogenesis of benign and malignant human prostatic tumors, *i.e.* benign prostatic hyperplasia and prostate cancer, thought to originate from different zones of the prostate [the transition zone (TZ) and peripheral zone (PZ), respectively]. Here, we examined the cellular distribution of ERα and ERβ in human normal and hyperplastic prostate tissues, using *in situ* hybridization and immunohistochemistry. ERα expression was restricted to stromal cells of PZ. In contrast, ERβ was expressed in the stromal cells of PZ as well as TZ. ERβ-positive epithelial cells were evenly distributed in PZ and TZ of the prostate. Our results suggest that estrogen may play a crucial role in the pathogenesis of benign prostatic hyperplasia through ERβ. (*J Clin Endocrinol Metab* 88: 1333–1340, 2003)

THE HUMAN PROSTATE is a sex hormone target organ, and both benign prostatic hyperplasia (BPH) and prostate cancer (PC) could develop in this organ. In fact, about 50% of men 51–60 yr old and 90% of men over 80 yr of age show histological evidence of BPH (1), and suffer from various urinary symptoms. Because these diseases are sex-hormone-sensitive, patients are often treated with antiandrogens or estrogens (2, 3). Although a number of studies have reported that certain sex hormones, such as androgens and estrogens, stimulate prostatic cell proliferation in experimental animal models, the role of cell proliferation in the progression of human BPH has not been established yet, because only a few proliferating cells are usually detected in the tissue (4). Thus, our understanding of the involvement of sex hormone in the pathogenesis of BPH is still only limited.

The prostate is absolutely dependent on androgens to maintain its size and secretory function (5). Although the androgen-dependency of the prostate gland has long been known, the role of estrogen in the prostate has been only recently recognized. In canine studies, castrated dogs showed regrowth and normal function after administration of exogenous androgens. When estrogens were added to the treatment protocol, the dogs developed glandular hyperplastic prostate, including an increase in total cell number (6). In other studies, pharmacological doses of estrogens induced a marked proliferative response of prostatic glandular epithelium (termed: squamous metaplasia) in a variety of mammals, including human (7).

Whereas serum estrogen levels are low in healthy men [approximately half the levels in nonpregnant women (8)], serum and intraprostatic estradiol levels (both absolute levels and those relative to testosterone) increase in men with age, accompanied by an increase in the prostate volume (9–11). In addition, patients with larger volumes of BPH tend to have high levels of serum estradiol (12). Therefore, the estrogen-dominant status in men after middle age has been implicated in the induction and progression of BPH (10). However, the molecular mechanism of estrogen action in the development of human BPH is largely unknown.

Estrogens require the presence of estrogen receptors (ERs) for their actions. ERs belong to a nuclear receptor superfamily of ligand-activated transcription factors; and, at present, two types of ERs (ERα and ERβ) have been characterized (13–16). ERα was known as ER before the discovery of ERβ, and its distribution has been thoroughly investigated in various human organs, including prostate and endometrium, breast cancer cells, and ovarian interstitial cells, which contain mostly ERα (17–20). ERα has been detected in stromal cells of human prostate, although the cellular localization of ERα remains controversial. At present, estrogen is thought to act indirectly on glandular cell proliferation, through ERα-positive stromal cells, in a paracrine manner (21).

ERβ has been recently cloned in the rat prostate and human testis (15, 16). ERα and ERβ share very high amino acid homology in the DNA binding domain, at 96%, but only show 53% homology in the ligand binding domain, as reported previously (22). The distribution of ERα and ERβ is variable, depending on tissues. In human, the testis contains mostly ERβ, and this subtype is also present in a variety of tissues, including kidney, interstitial mucosa, lung parenchyma, bone marrow, bone, brain, endothelial cells, and prostate gland (23). Although the biological action of ERβ in human prostate remains to be clarified, ERβ knockout mice develop prostatic hyperplasia with aging, suggesting that ERβ may play an important role in the development of BPH

Abbreviations: AR, Androgen receptor; BPH, benign prostatic hyperplasia; DAB, 3,3′-diaminobenzidine/4HCl; ER, estrogen receptor; HRP, horseradish peroxidase; IHC, immunohistochemistry; ISH, *in situ* hybridization; PC, prostate cancer; PZ, peripheral zone; SSC, standard saline citrate; TZ, transition zone.

(24, 25). At present, however, there are conflicting reports on the cellular localization of ERβ in human prostate. Enmark *et al.* (26) and Bonkhoff *et al.* (27) demonstrated that ERβ expression was only marginal or absent in human prostate. On the other hand, using immunohistochemistry (IHC), Royuela *et al.* (19) reported that ERβ was significantly expressed and localized only in the nuclei of the basal cells, whereas others detected a similar expression in the nuclei of stromal cells as well as the basal cells and also the cytoplasm of glandular epithelial cells by IHC (20, 28). Considering that the results of IHC are often influenced by the stability of the epitope and fixation procedure, analysis of ERβ transcript by *in situ* hybridization (ISH) would be appropriate to resolve the controversy.

According to zonal anatomy described by McNeal *et al.* (29, 30), all BPH nodules and most PC foci arise in the transition zone (TZ) and the peripheral zone (PZ). To our knowledge, there are no studies that have examined the zonal differences, if any, in the expression of ERα and ERβ and whether such difference may reflect the pathogenesis of these prostatic diseases. In the present study, we first examined the cellular distribution of ERβ mRNA and protein in normal human prostate tissues, using nonradioactive ISH and IHC, respectively. The antibody for ERβ was raised by immunizing rabbits with a synthetic peptide of a part of the C-terminal domain of human ERβ (22), and the specificity of this antibody was confirmed by Western blot analysis. We then investigated the expression of ERα and ERβ in human BPH tissues, by IHC, focusing on the difference between PZ and TZ. Our results revealed a discrete cellular distribution of ERs and that such distribution varied between the TZ and PZ, suggesting that the differential expression of ERα and ERβ may be involved in the pathogenesis of prostatic diseases, especially BPH. Our results also indicated that the zone-dependent staining for ERα and ERβ may explain, at least partly, the discrepancy for the distribution of ERs.

Materials and Methods

Chemicals and biochemicals

DAB (3,3'-diaminobenzidine/4HCl) was purchased from Dojin Chemical Co. (Kumamoto, Japan). SDS-PAGE was purchased from Daiichi Pure Chemicals Company Ltd. (Tokyo, Japan). Immobilon, polyvinylidene difluoride membranes, was purchased from Millipore Corp. (Bedford, MA). The enhanced chemiluminescence system was purchased from Amersham International (Buckinghamshire, UK). Yeast tRNA, salmon testicular DNA, BSA, Brij 35, Tween 20, and 3-aminopropyltriethoxysilane were purchased from Sigma (St. Louis, MO). Formamide was purchased from Nacalai Tesque (Kyoto, Japan).

Antibodies

Antiserum against human ERβ was obtained from a rabbit immunized with this peptide conjugated to keyhole limpet hemocyanin, as described previously (31). The synthetic oligopeptide sequence (511-CSPAEDSKSKEGSQNPQSQ-530) corresponding to the C-terminal amino acid residues of human ERβ (22) was selected. When the titer of antibody reached a plateau, the entire peripheral blood was drawn, and the serum was separated. The experimental protocol was approved by the Ethics Review Committee for Animal Experimentation of Nagasaki University School of Medicine.

Mouse monoclonal antihuman ERα IgG1 (1D5), normal goat serum, and normal rabbit serum were purchased from DAKO Corp. (Glostrup, Denmark). Mouse monoclonal antihuman androgen receptor (AR) IgG1 (NCL-AR-318) was purchased from Novocastra Laboratories (Newcastle, UK). Horseradish peroxidase (HRP)-conjugated goat antirabbit IgG F(ab')$_2$ was purchased from MBL (Nagoya, Japan). HRP-conjugated goat antimouse IgG F(ab')$_2$ was purchased from Chemicon International (Temecula, CA). Normal goat IgG and normal mouse IgG were purchased from Sigma. HRP-conjugated mouse monoclonal anti-T-T IgG was from Kyowa Medex (Tokyo, Japan).

All other reagents used in this study were from Wako Pure Chemical Industries Ltd. (Osaka, Japan) and were of analytical grade.

Tissue collection and preparation

Prostate tissues were obtained from 16 patients: 10 prostatic needle biopsy specimens (age, 55–75 yr) and 6 radical cystoprostatectomized prostates (age, 56–67 yr) from patients with primary muscle-invasive bladder cancer. Eleven of these tissues were diagnosed clinically and histopathologically as BPH, whereas the remaining 5 were normal. All specimens were obtained from patients at the Department of Urology, Nagasaki Atomic Bomb Hospital, in 2001. None of the patients had received any treatment before tissue sampling. The specimens of needle prostatic biopsies were obtained by the transperineal approach, under the guidance of transrectal ultrasonography. On the other hand, the samples of PZ or TZ were also taken from radical cystoprostatectomy, under direct vision. Some sections from all specimens were stained with hematoxylin and eosin for pathological examination to confirm the absence of PC and prostatic intraepithelial neoplasia.

For Western blot analysis, prostate tissue specimens (obtained from radical cystoprostatectomy) and human testis (obtained from patients with orchiectomy) for PC treatment were cut into several small pieces and rapidly frozen in liquid nitrogen and later used for the extraction of protein. For IHC, all prostatic samples were fixed with 10% neutral buffered formalin and embedded in paraffin using a standard procedure. The specimens were cut serially into 5-μm-thick sections and mounted on 3-aminopropyltriethoxysilane-coated glass slides.

IHC for ERα, ERβ, and AR

We used indirect enzyme-IHC for detection of ERα, ERβ, and AR. For IHC of ERβ, paraffin sections were dewaxed with toluene and rehydrated by serial graded ethanol solutions. Then the sections were microwaved at 95 C for 20 min in 10 mM citrate buffer (pH 6.0). The following protocol was essentially similar to that previously established for rabbit polyclonal antibody (31). Briefly, after washing the sections with PBS, endogenous peroxidase activity was inhibited by immersing the slides in 0.3% H_2O_2 in methanol for 30 min. After the slides were washed with PBS again, they were preincubated with 10% normal goat serum and 1% BSA in PBS for 1 h to reduce nonspecific binding of antibodies. Then, the sections were reacted overnight with anti-ERβ antiserum at a dilution of 1:400. After washing with 0.075% Brij 35 in PBS and rinsing with PBS, the sections were incubated with HRP-labeled goat antirabbit IgG F(ab')$_2$ at a 1:200 dilution for 1 h. After washing with 0.075% Brij 35 in PBS and rinsing with PBS, the sites of HRP were visualized by DAB and H_2O_2. The sections were counterstained with Mayer's hematoxylin. As a control, some sections were reacted with normal rabbit serum instead of the specific antiserum, at the same concentration.

For IHC of ERα and AR, paraffin sections were processed in a manner similar to that described above. After preincubation with 500 μg/ml normal goat IgG and 1% BSA in PBS for 1 h, the sections were reacted with mouse monoclonal anti-ERα IgG1 at a dilution of 1:200 and anti-AR IgG1 at a dilution of 1:50 overnight. After washing with 0.075% Brij 35 in PBS and rinsing with PBS, sections were incubated with HRP-labeled goat antimouse IgG F(ab')$_2$ at a dilution 1:100 for 1 h. After washing in 0.075% Brij 35 in PBS and rinsing in PBS, the sites of HRP were visualized with DAB and H_2O_2 and then counterstained with Mayer's hematoxylin. As a negative control, some sections were reacted with normal mouse IgG instead of the specific primary antibody, at the same concentration.

The frequency of positive cells for ERβ, ERα, and AR was graded as negative (−), occasionally positive (+), often positive (++), and abundantly positive (+++), relative to the background staining with normal rabbit serum or normal mouse IgG.

To confirm the zonal difference of ERβ expression in the stroma of BPH specimens, the proportion of ERβ-positive cells in the stroma of both PZ and TZ was calculated by counting at least 1000 cells at ×400

magnification. A computer software package, StatView 4.5 (Abacus Concepts, Inc., Berkeley, CA), was used for statistical analysis. Data were expressed as mean ± SD. The difference in the proportion of ERβ-positive stromal cells between two prostatic zones was examined using the Mann-Whitney *U* test. A *P* value less than 0.05 indicated statistical significance.

Western blot analysis of ERβ

The frozen tissues were thawed and homogenized with a Polytron tissue homogenizer (Kinematica AG, Switzerland) in the lysis buffer consisting of 20 mM Tris-HCl (pH 7.4), 5 mM EDTA, 1 mM phenylmethylsulfonyl fluoride, 10 μg/ml aprotinin, 2 μg/ml leupeptin, 10% glycerol, and 1% Triton X-100 on ice. After homogenization and centrifugation at 15,000 rpm for 30 min at 4 C, the supernatant was collected and then stored at −80 C.

Before Western blot analysis, the protein concentration was determined by the method of Bradford (32) using BSA as a standard. Then, an aliquot (10 μg) of the lysates was mixed with the loading buffer [consisting of 250 mM Tris-HCl (pH 6.8), 30% glycerol, 0.01% bromophenol blue, 2% SDS and 10% 2-mercaptoethanol], boiled for 5 min, and separated by SDS-PAGE with 4–20% gradient gel. After electrophoretic transfer onto polyvinylidene difluoride membranes, the membranes were incubated with PBS containing 5% nonfat dry milk and 5% BSA, to reduce nonspecific binding of antibodies for 1 h. Then the membranes were reacted overnight with anti-ERβ antiserum at a dilution of 1:2000. After washing with 0.2% Tween 20 in PBS, the membranes were reacted with HRP-conjugated goat antirabbit IgG $F(ab')_2$ at a dilution 1:3000 for 1 h. Finally, after washing with 0.2% Tween 20 in PBS, the bands were visualized by an enhanced chemiluminescence system.

Preparation of oligo-DNA probes for ERβ

A 45-base sequence complementary to ERβ mRNA (nucleotide no. 861–905) was selected. These antisense and sense sequences were synthesized together with two and three TTA repeats, at the 5′- and 3′-ends of sequences, and used as probes after haptenization with T-T dimer, as detailed previously (33). The sequences of antisense and sense probes used in this study were 5′-TTATTACACTAGCTGCTCGGGGCTCAGGGCGTCCAGCAGCAGCTCCCGCACATTATTATT-3′ and 5′-TTATTAGTGCGGGAGCTGCTGCTGGACGCCCTGAGCCCCGAGCAGCTAGTGATTATTATT-3′, respectively. A computer-assisted search of GenBank of the above antisense sequences, as well as sense sequences, showed no significant homology with any known sequences. The T-T dimer was introduced into oligo-DNAs by UV irradiation (254 nm) using a dose of 12,000 J/m^2. The generation of T-T dimer was verified immunochemically using a mouse monoclonal anti-T-T IgG.

Dot-blot hybridization

Unless otherwise specified, all procedures were conducted at room temperature (20–25 C) throughout the experiment. Two-microfilter drops of the sense oligo-DNA solution were pipetted onto nitrocellulose membranes that had been pretreated with 20× standard saline citrate (SSC) [1× SCC; 0.015 M sodium citrate (pH 7.0) supplemented with 0.15 M sodium chloride] in series of spots at 1 pg to 10 ng/spot. The procedure of dot-blot hybridization has been described previously (34). Briefly, after air-drying, the filters were baked at 80 C for 2 h and incubated at 37 C for 2 h with prehybridization medium. The membranes were hybridized overnight at 37 C with 1 μg/ml T-T-dimerized oligo-DNA probe in hybridization medium. After hybridization, the membranes were immersed for 1 h in a blocking solution that contained 5% BSA, 500 μg/ml normal mouse IgG, 100 μg/ml yeast tRNA, and 100 μg/ml salmon testicular DNA in PBS. The reaction with HRP-linked mouse monoclonal anti-(T-T dimer) IgG at a 1:80 dilution was conducted at least for 3 h. The membranes were then washed with 0.075% Brij 35 in PBS for 1 h, and the sites of HRP were visualized using a chromogen solution containing DAB, H_2O_2, $CoCl_2$, and $NiSO_4(NH_4)_2SO_4$ (35).

ISH for ERβ

Nonradioactive ISH was performed according to the method described previously (33, 34). Briefly, sections were deparaffinized and rehydrated using standard procedures. This was followed by treatment with 0.3% H_2O_2 in methanol for 15 min to inhibit endogenous peroxidase activity, 0.2 N HCl for 20 min and 100 μg/ml proteinase K at 37 C for 15 min. After postfixation with 4% paraformaldehyde in PBS for 5 min, the sections were immersed in 2 mg/ml glycine in PBS for 30 min and kept in 40% deionized formamide in 4× SSC until used for hybridization. Hybridization was carried out for 12 h at 37 C with 2 μg/ml T-T-dimerized antisense oligo-DNA for ERβ dissolved in the hybridization medium as described above. Then, the slides were washed with 50% formamide in 2× SSC, followed by 2× SSC. The signals were detected immunohistochemically, as described above. To evaluate the specificity of ERβ mRNA signal, consecutive tissue sections were hybridized with T-T-dimerized ERβ sense oligo-DNA as a negative control. Furthermore, the integrity of tissue RNA was assessed with T-T-dimerized 28S rRNA complementary probe (36).

Results

Immunohistochemical localization of ERα, ERβ, and AR in hyperplastic prostates

We presented here the results of a typical case with BPH or its PZ normal part (Figs. 1 and 2). The histological examinations revealed epithelial hyperplasia of TZ and normal appearance of PZ (Figs. 1A and 2A).

In all specimens, ERα was consistently detected in the nuclei of stromal cells. However, ERα-positive stromal cells were predominantly observed in PZ, but not in TZ, in normal and BPH tissues (Figs. 1B and 2B). Thus, there was a clear difference in ERα expression patterns between PZ and TZ, where the epithelial cells, basal cells, endothelial cells, and vascular smooth muscle cells were all negative for ERα.

On the other hand, a moderate staining for ERβ was detected in the nuclei of some but not all, epithelial and stromal cells, whereas it was strong in the nuclei of basal cells in normal and hyperplastic tissues, as shown in Figs. 1C and 2C. Interestingly, it should be noted that the staining for ERβ in the glandular epithelial cells was found in the perinuclear as well as nuclear regions. The difference in the staining intensity for ERβ between TZ and PZ was found in the stromal cells but not in the epithelial cells. The signal for ERβ in the stromal cells of PZ is stronger than that of TZ. Although there was no difference in the cellular localization of ERβ between PZ and TZ in BPH tissues, the number of ERβ-positive cells was clearly less in the stroma of TZ than that of PZ. Quantitative analysis showed that the percentage of ERβ-positive stromal cells in PZ (74.9 ± 9.0%) was significantly higher than in TZ (22.7 ± 8.9%, $P < 0.0001$, Mann-Whitney *U* test), whereas there was no difference in the percentages of ERβ-positive cells of both glandular epithelial cells and basal cells between PZ and TZ.

In contrast, AR was consistently found in the nuclei of glandular epithelial cells, as well as in many stromal cells and some basal cells. Also, the nuclear staining in the basal cells was less intense than that of glandular epithelial cells. There was no difference in the expression of AR between PZ and TZ in BPH tissues, as shown in Figs. 1D and 2D. In addition, there was no significant variation in the expression of ERα, ERβ, and AR among BPH specimens, as summarized in Table 1.

When the primary antibodies were replaced with normal rabbit IgG or normal mouse IgG, no staining was observed (Figs. 1, E and F; and 2, E and F).

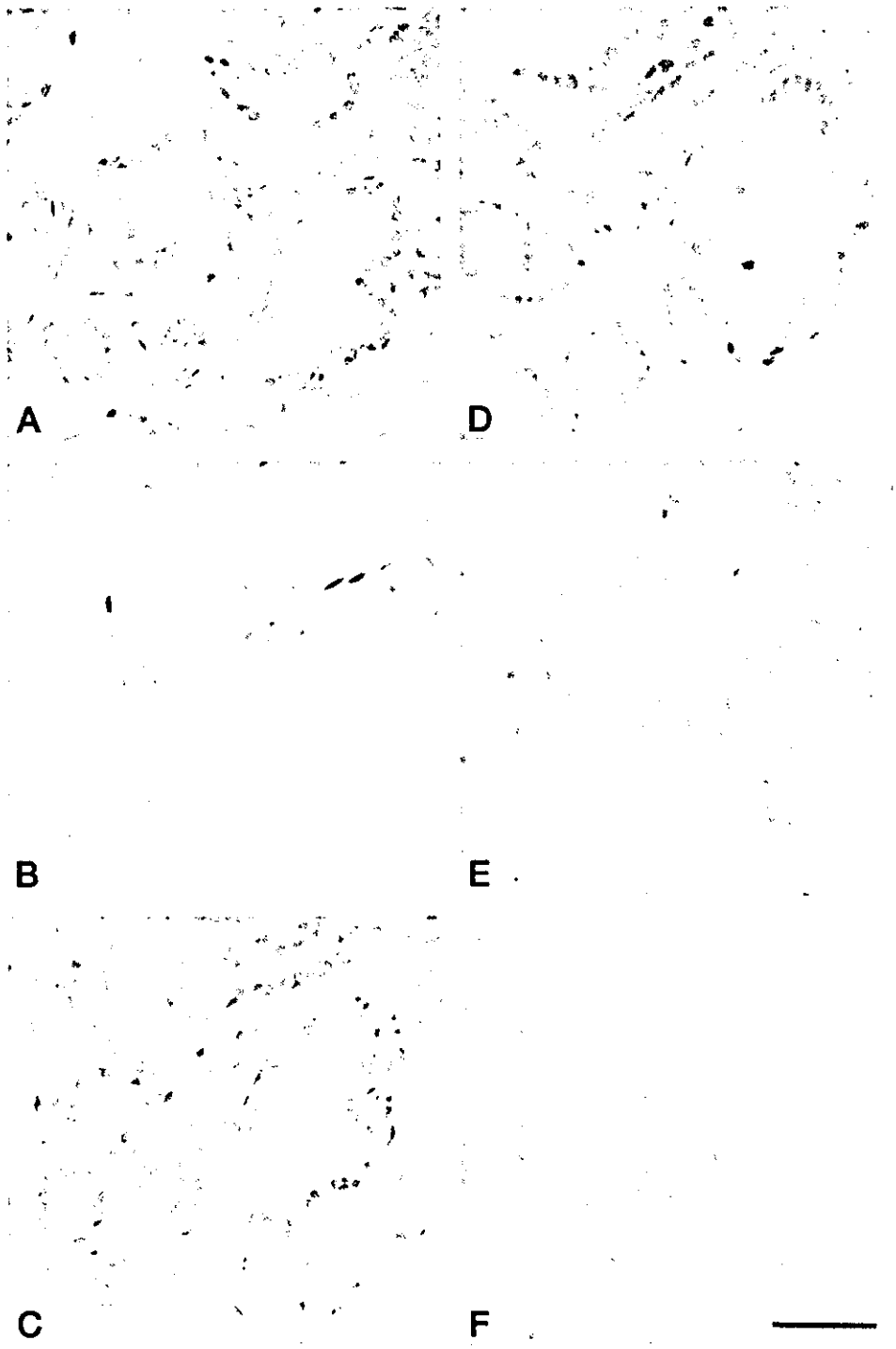

FIG. 1. Expression of ERα, ERβ, and AR in the PZ of representative BPH tissue samples. A, Hematoxylin and eosin staining. B, Immunostaining for ERα. ERα is expressed in stromal cells. C, Immunostaining for ERβ. ERβ is expressed in the nuclei of both epithelial cells and some stromal cells. The signal in both basal cells and stromal cells is stronger than that of glandular epithelial cells. D, Immunostaining for AR. AR was consistently found in the nuclei of glandular epithelial cells, as well as in many stromal cells and some basal cells. Also, the nuclei of basal cells are less intense than those of glandular epithelial cells. E, Negative control for ERβ immunostaining by incubation with normal rabbit serum. F, Negative controls for both ERα and AR immunostaining by incubation with normal mouse IgG. *Scale bar*, 50 μm; original magnification, ×200.

Evaluation of specificity of immunohistochemical results with anti-ERβ antiserum

Western blot analysis of ERβ. To confirm the specificity of the newly raised antiserum for human ERβ, we performed Western blotting, using the lysate from human testis (lane 1, Fig. 3), which is known to express ERβ (16). As shown in Fig. 3, a band of approximately 60 kDa was detected with the ERβ antiserum. When the lysates from normal prostate tissues were analyzed by the ERβ antiserum (lane 2), we also detected at least three bands (approximately 60-, 57-, and 53-kDa). The results may indicate the presence of several ERβ splicing isoforms that have been found in the human prostate (22, 37). When the antiserum was replaced with normal rabbit serum, no bands were observed (lane 3).

ISH of ERβ. As shown in Fig. 4, when ERβ sense oligo-DNA, fixed onto a nitrocellulose membrane at various amounts, was hybridized with T-T-dimerized ERβ antisense oligo-DNA or T-T-dimerized ERβ sense oligo-DNA, as little as 1

FIG. 2. Expression of ERα, ERβ, and AR in the TZ of representative BPH tissue samples. A, Hematoxylin and eosin staining. B, Immunostaining for ERα. Note the lack of signal of ERα. C, Immunostaining for ERβ. ERβ is expressed in the nuclei of both epithelial cells and a few stromal cells. Especially, the signal in basal cells is very intense. D, Immunostaining for AR. AR was consistently found in the nuclei of glandular epithelial cells, as well as in many stromal cells and some basal cells. However, the nuclei of basal cells are less intense than those of glandular epithelial cells. E, Negative control for ERβ immunostaining by incubation with normal rabbit serum. F, Negative controls for both ERα and AR immunostaining by incubation with normal mouse IgG. *Scale bar*, 50 μm; original magnification, ×200.

TABLE 1. Semiquantitative analysis of cellular distribution of ERα, ERβ, and AR in specimens of BPH determined by IHC

	ERα	ERβ	AR
PZ			
Glandular epithelial cells	−	+	+++
Basal cells	−	+++	+
Stromal cells	++	+++	++
TZ			
Glandular epithelial cells	−	+	+++
Basal cells	−	+++	+
Stromal cells	−	+	++

Signal intensity: −, non; +, occasionally; ++, often; +++, abundantly.

pg ERβ sense DNA was detected with the antisense probe, but no signal was detected with the sense oligo-DNA. These results indicated that the antisense probe synthesized in our laboratory was specific, with adequate sensitivity to be useful in ISH studies.

For the ISH study of mRNA, because it is important to determine the RNA integrity and preservation in target tissues, we first confirmed the preservation of RNA in all specimens by performing ISH for 28S rRNA using T-T-dimerized 28S rRNA-complementary oligo-DNA. A typical case with fibroadenomatous hyperplasia was demonstrated (Fig. 5A), and the staining for 28S rRNA was detected in the cytoplasm area as well as nucleoli, as shown in Fig. 5B. Further analysis of ERβ mRNA expression in normal and hyperplastic prostate showed strong expression of ERβ mRNA in most of the glandular epithelial cells, basal cells, and some stromal cells and that such staining pattern was not influenced anatomically, *i.e.* TZ and PZ. The signal for ERβ mRNA was localized to the perinuclear area of the cytoplasm (Fig. 5C). The cellular distribution of the signal for ERβ mRNA seemed to be essentially similar to that of ERβ protein by IHC. As a negative control, adjacent sections were hybridized with

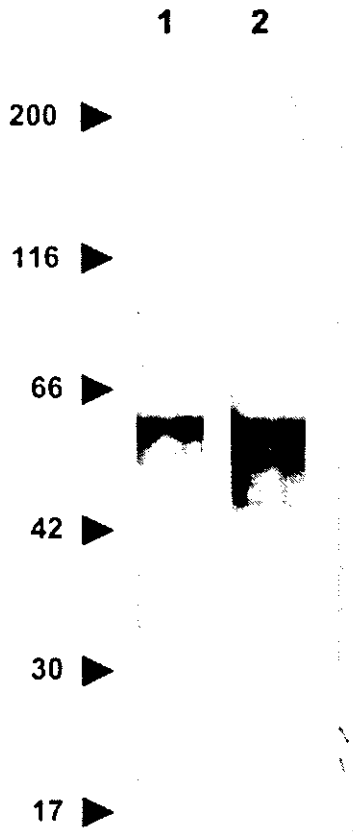

FIG. 3. Western blot analysis of ERβ. Each of the 10-μg extracts from the human testis and prostates was subjected to SDS-PAGE. Western blotting was performed using ERβ antiserum. Lane 1, Human testis; lane 2, human prostate; lane 3, using normal rabbit serum, as a negative control. At least three bands (approximately 60-, 57-, and 53-kDa) were detectable.

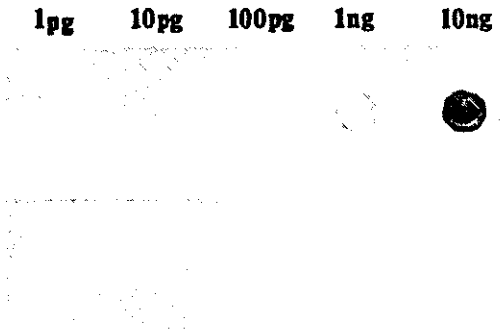

FIG. 4. Colorimetric dot-blot hybridization. Various amounts (1 pg–10 ng/spot) of ERβ sense oligo-DNA, which were fixed onto nitrocellulose membranes, were hybridized with the T-T-dimerized antisense oligo-DNA (*top*) or the T-T-dimerized sense oligo-DNA (*bottom*). At least, 1 pg DNA was detected.

the T-T-dimerized ERβ sense oligo-DNA probe, resulting in no staining (Fig. 5D).

Discussion

In the present study, we examined zonal expression of ERα and ERβ in human normal and hyperplastic prostates, and we found that ERα was expressed only in the stromal cells of PZ but not of TZ. In contrast, ERβ expression was detected in a wide variety of prostate cells, including glandular epithelial cells, basal cells, and stromal cells; and more importantly, the proportion of ERβ-positive cells was significantly higher in the stroma of PZ than that of TZ. Considering that BPH nodules develop from the TZ, these results seem to indicate that ERβ, rather than ERα, may be preferentially involved in the pathogenesis of BPH.

During the past decade, conflicting results were reported regarding the localization of ERα in human prostate tissue. In fact, a number of investigators, including our group, found both ERα mRNA and its protein in stromal cells only (18, 19), whereas other groups found ERα protein in some basal epithelial cells as well as stromal cells (17, 20, 27). Such discrepancies are poorly understood and are considered to be attributable to methodological differences. The present findings of zonal distribution of ERα in human prostate offer an alternative explanation for the discrepancies; ERα could not be detected in BPH specimens that were removed from TZ by open prostatectomy, whereas specimens of PC were positive for ERα expression.

In the present study, we also investigated the expression of ERβ in human prostate tissues by IHC and ISH, and we found differences in the percentages of ERβ-positive cells in the stroma between TZ and PZ. These results contradict those of Leav *et al.* (20), who recently reported the lack of difference in ERβ expression among central zone, TZ, and PZ. Although the reason for the discrepancy is not known at present, the roles of ERβ-positive stromal cells in TZ should be of interest for a better understanding of the pathogenesis of BPH.

In a variety of tissues, including prostate gland, estrogens were thought to act on the induction of glandular epithelial cell proliferation, through ERα-positive stromal cells, in a paracrine fashion (23). However, we could not find ERα expression in the TZ, where BPH nodules develop. In addition, it is now known that there was no prostatic abnormality in ERα knockout mice (38), and there was also no special mention of clinical features related to prostatic hyperplasia in a patient reported to lack functional ERα (39). Therefore, we favor the notion that ERα may not be involved in the pathogenesis of human BPH. On the other hand, ERα expression was restricted to the stromal cells of PZ, which is supposed to be the origin site of PC. In addition, ERα was localized in the nuclei of both many cancer cells and its surrounding stromal cells in PC tissues (18–20, 27, 40). Considering that estrogens are involved in cancer development, by stimulation of cell proliferation, in a variety of tumors, including PC (41), ERα (rather than ERβ) may be also implicated in both development and progression of PC (26, 42).

Moreover, the finding that ERβ knockout mice develop prostatic hyperplasia with aging strongly indicates that ERβ may play a negative role in the regulation of glandular epithelial cell proliferation in the prostate (24, 43). In fact, ERβ is abundantly expressed in the glandular cells and basal cells of hyperplastic tissues (19, 25); but to date, there is no report on the role of ERβ in the growth of normal human prostate. In addition, the expression of ERβ was reduced in high-grade dysplasia, compared with that of normal prostate gland and lower grade lesions, and the ERβ-positive cells in human PC

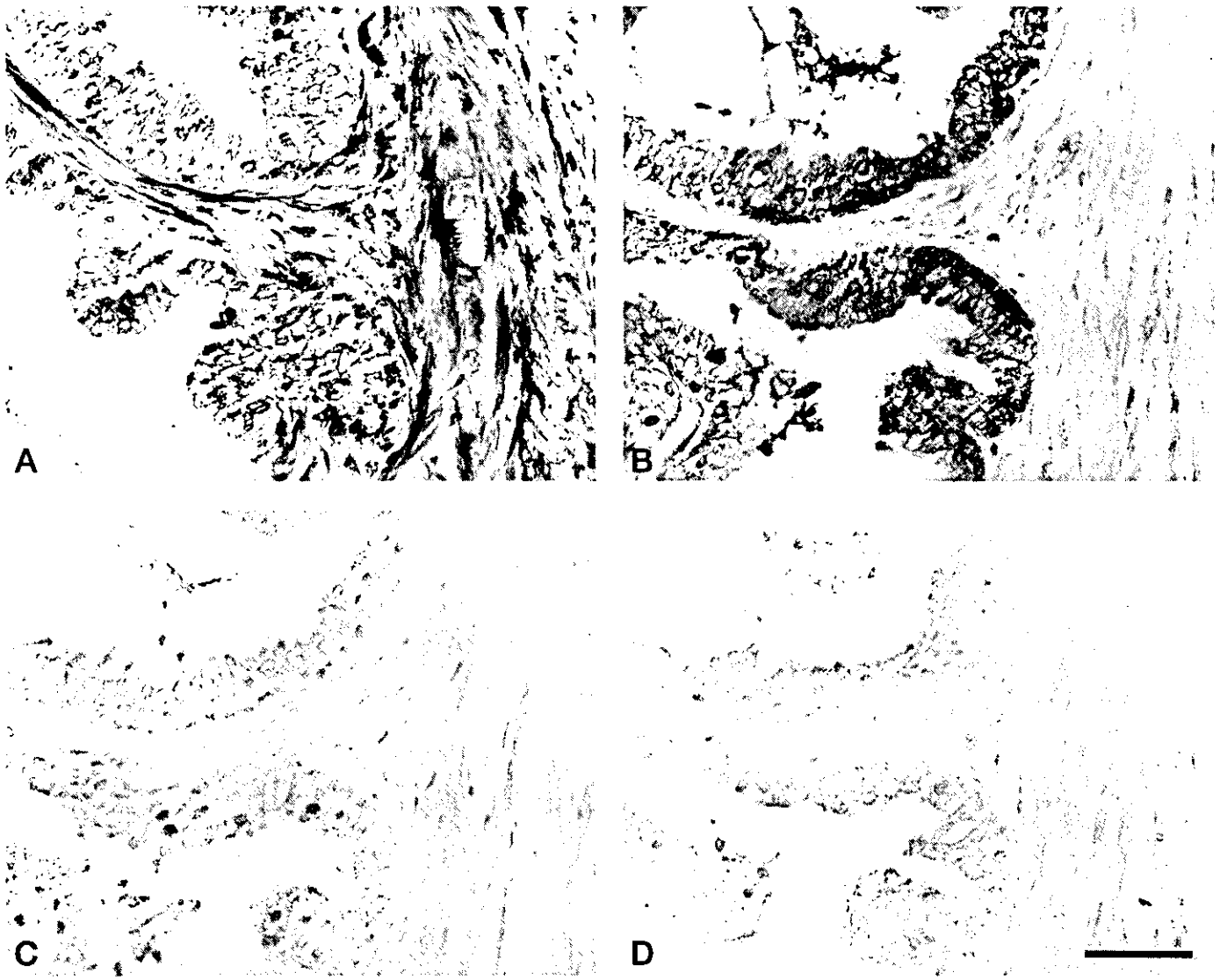

FIG. 5. ERβ mRNA expression in benign prostate tissue using nonradioactive ISH. A, Hematoxylin and eosin staining. B, 28S rRNA antisense probe, as a positive control. C, ERβ antisense probe. ERβ mRNA was expressed strongly in glandular epithelial cells, basal cells, and some stromal cells. Note the localization of staining to the cytoplasm of ERβ mRNA-positive cells, especially the perinuclear area of the cytoplasm. D, ERβ mRNA sense probe, as a negative control. *Scale bar*, 50 μm; original magnification, ×200.

tissues decreased with tumor grading or was absent (20, 28). In addition, ERβ expression was lost in most of the human PC specimens, because of the inactivation of the ERβ gene through CpG methylation of the promoter region of this gene (44). Therefore, these findings seem to suggest that ERβ may protect glandular epithelial cells against abnormal growth in human prostate (44, 45).

Interestingly, the strongest staining for ERβ was observed in the basal cells, in accordance with the findings by Leav *et al.* (20). In fact, it has been noticed that the basal cells have quite different biological properties from those of the glandular epithelial cells, particularly with respect to proliferation potential and steroidogenesis, and may play a crucial role in the prostatic carcinogenesis (46, 47). Therefore, we speculate that the ERβ-positive basal cells may directly modulate the growth of themselves by estrogen via ERβ. Moreover, AR is expressed not only in the basal cells but also in both the stromal and glandular epithelial cells. Because the basal cell proliferation is supposed to be antagonized by the purported growth-inhibitory action of ERβ expressed in basal cells as well as stromal cells (20, 24, 25), it may be stimulated through adjacent AR- and ERα-positive cells. Therefore, we propose that the environment in the stroma of TZ, where ERβ expression is low, may be favorable for cell proliferation and the development of BPH.

Finally, we have demonstrated, in the present study, a differential expression of ERα and ERβ between TZ and PZ of human hyperplastic prostate, suggesting that estrogen may play a crucial role in the pathogenesis of BPH through ERβ. In addition, we propose that the environment in the stroma of TZ, where ERβ expression is low, may be favorable for the cell proliferation and the development of BPH.

Acknowledgments

Received July 5, 2002. Accepted November 25, 2002.

Address all correspondence and requests for reprints to: Takehiko Koji, Ph.D., Department of Histology and Cell Biology, Nagasaki University School of Medicine, 1-12-4 Sakamoto, Nagasaki 852-8523, Japan. E-mail: tkoji@net.nagasaki-u.ac.jp.

This work was supported in part by a Grant-in-Aid for Scientific Research from the Japanese Ministry of Education, Science, Sports and Culture (no. 1247003; to T.K.) and by a grant from the Japanese Environment Agency (to T.K.).

References

1. **Berry SJ, Coffey DS, Walsh PC, Ewing LL** 1984 The development of human benign prostatic hyperplasia with age. J Urol 132:474–479
2. **Lepor H** 1989 Nonoperative management of benign prostatic hyperplasia. J Urol 141:1283–1289
3. **Cox RL, Crawford ED** 1995 Estrogens in the treatment of prostate cancer. J Urol 154:1991–1998
4. **McConnell JD** 1998 Epidemiology, etiology, pathophysiology, and diagnosis of benign prostatic hyperplasia. In: Walsh PC, Retik AB, Vaughan Jr ED, Wein AJ, eds. Campbell's urology. 7th ed. Philadelphia: WB Saunders Co; 1429–1452
5. **Taplin ME, Ho SM** 2001 The endocrinology of prostate cancer. J Clin Endocrinol Metab 86:3467–3477
6. **Walsh PC, Wilson JD** 1976 The induction of prostatic hypertrophy in the dog with androstanediol. J Clin Invest 57:1093–1907
7. **Levine AC, Kirschenbaum A, Droller M, Gabrilove JL** 1991 Effect of the addition of estrogen to medical castration on prostatic size, symptoms, histology and serum prostate specific antigen in 4 men with benign prostatic hypertrophy. J Urol 146:790–794
8. **Isidori AM, Strollo F, More M, Caprio M, Aversa A, Moretti C, Frajese G, Riondino G, Fabbri A** 2000 Leptin and aging: correlation with endocrine changes in male and female healthy adult populations of different body weights. J Clin Endocrinol Metab 85:1954–1962
9. **Rubens R, Dhont M, Vermeulen A** 1974 Further studies on Leydig cell function in old age. J Clin Endocrinol Metab 39:40–45
10. **Shibata Y, Ito K, Suzuki K, Nakano K, Fukabori Y, Suzuki R, Kawabe Y, Honma S, Yamanaka H** 2000 Changes in the endocrine environment of the human prostate transition zone with aging: simultaneous quantitative analysis of prostatic sex steroids and comparison with human prostatic histological composition. Prostate 42:45–55
11. **Seppelt U** 1978 Correlation among prostate stroma, plasma estrogen levels, and urinary estrogen excretion in patients with benign prostatic hypertrophy. J Clin Endocrinol Metab 47:1230–1235
12. **Partin AW, Oesterling JE, Epstein JI, Horton R, Walsh PC** 1991 Influence of age and endocrine factors on the volume of benign prostatic hyperplasia. J Urol 145:405–409
13. **Hobisch A, Hittmair A, Daxenbichler G, Wille S, Radmayr C, Hobisch-Hagen P, Bartsch G, Klocker H, Culig Z** 1997 Metastatic lesions from prostate cancer do not express oestrogen and progesterone receptors. J Pathol 182: 365–361
14. **Walter P, Green S, Greene G, Krust A, Bornert JM, Jeltsch JM, Staub A, Jensen E, Scrace G, Waterfield M, Chambon P** 1985 Cloning of the human estrogen receptor cDNA. Proc Natl Acad Sci USA 82:7889–7893
15. **Kuiper GG, Enmark E, Pelto-Huikko M, Nilsson S, Gustafsson JA** 1996 Cloning of a novel estrogen receptor expressed in rat prostate and ovary. Proc Natl Acad Sci USA 93:5925–5930
16. **Mosselman S, Polman J, Dijkema R** 1996 ERβ: identification of a novel human estrogen receptor. FEBS Lett 392:49–53
17. **Schulze H, Claus S** 1990 Histological localization of estrogen receptors in normal and diseased human prostates by immunocytochemistry. Prostate 16:331–343
18. **Ehara H, Koji T, Deguchi T, Yoshii A, Nakano M, Nakane PK, Kawada Y** 1995 Expression of estrogen receptor in diseased human prostate assessed by non-radioactive in situ hybridization and immunohistochemistry. Prostate 27: 304–313
19. **Royuela M, de Miguel MP, Bethencourt FR, Sanchez-Chapado M, Fraile B, Arenas MI, Paniagua R** 2001 Estrogen receptor α and β in the normal, hyperplastic and carcinomatous human prostate. J Endocrinol 168:447–454
20. **Leav I, Lau KM, Adams JY, McNeal JE, Taplin ME, Wang J, Singh H, Ho SM** 2001 Comparative studies of the estrogen receptors β and α and the androgen receptor in normal human prostate glands, dysplasia, and in primary and metastatic carcinoma. Am J Pathol 159:79–92
21. **International Prostate Health Council Study Group** 2000 Estrogens and prostatic disease. Prostate 45:87–100
22. **Ogawa S, Inoue S, Watanabe T, Hiroi H, Orimo A, Hosoi T, Ouchi Y, Muramatsu M** 1998 The complete primary structure of human estrogen receptor β (hERβ) and its heterodimerization with ER α *in vivo* and *in vitro*. Biochem Biophys Res Commun 243:122–126
23. **Gruber CJ, Tschugguel W, Schneeberger C, Huber JC** 2002 Production and actions of estrogens. N Engl J Med 346:340–352
24. **Krege JH, Hodgin JB, Couse JF, Enmark E, Warner M, Mahler JF, Sar M, Korach KS, Gustafsson JA, Smithies O** 1998 Generation and reproductive phenotypes of mice lacking estrogen receptor β. Proc Natl Acad Sci USA 95:15677–15682
25. **Lau K-M, LaSpina M, Long J, Ho S-M** 2000 Expression of estrogen receptor (ER)-α and ER-β in normal and malignant prostatic epithelial cells: regulation by methylation and involvement in growth regulation. Cancer Res 60:3175–3182
26. **Enmark E, Pelto-Huikko M, Grandien K, Lagercrantz S, Lagercrantz J, Fried G, Nordenskjold M, Gustafsson JA** 1997 Human estrogen receptor β gene structure, chromosomal localization, and expression pattern. J Clin Endocrinol Metab 82:4258–4265
27. **Bonkhoff H, Fixemer T, Hunsicker I, Remberger K** 1999 Estrogen receptor expression in prostate cancer and premalignant prostatic lesions. Am J Pathol 155:641–647
28. **Pasquali D, Staibano S, Prezioso D, Franco R, Esposito D, Notaro A, Rosa GD, Bellastella A, Sinisi AA** 2001 Estrogen receptor β expression in human prostate tissue. Mol Cell Endocrinol 178:47–50
29. **McNeal JE** 1981 Normal and pathologic anatomy of prostate. Urology 17(Suppl):11–16
30. **McNeal JE** 1978 Origin and evaluation of benign prostatic enlargement. Invest Urol 15:340–345
31. **Nishihara E, Nagayama Y, Inoue S, Hiroi H, Muramatsu M, Yamashita S, Koji T** 2000 Ontogenic changes in the expression of estrogen receptor α and β in rat pituitary gland detected by immunohistochemistry. Endocrinology 141:615–620
32. **Bradford MM** 1976 A rapid and sensitive method for the quantification of microgram quantities of protein utilizing the principle of protein-dye binding. Anal Biochem 72:248–254
33. **Koji T, Nakane PK** 1996 Recent advances in molecular histochemical techniques: *in situ* hybridization and southwestern histochemistry. J Electron Microsc (Tokyo) 45:119–127
34. **Tsurusaki T, Koji T, Sakai H, Kanetake H, Nakane PK, Saito Y** 1998 Cellular expression of beta-microseminoprotein (β-MSP) mRNA and its protein in untreated prostate cancer. Prostate 35:109–116
35. **Adams JC** 1981 Heavy metal intensification of DAB-based HRP reaction product. J Histochem Cytochem 29:775
36. **Yoshii A, Koji T, Ohsawa N, Nakane PK** 1995 *In situ* localization of ribosomal RNAs in a reliable reference for hybridizable RNA in tissue sections. J Histochem Cytochem 43:321–327
37. **Moore JT, McKee DD, Slentz-Kesler K, Moore LB, Jones SA, Horne EL, Su JL, Kliewer SA, Lehmann JM, Willson TM** 1998 Cloning and characterization of human estrogen receptor β isoforms. Biochem Biophys Res Commun 247: 75–78
38. **Lubahn DB, Moyer JS, Golding TS, Couse JF, Korach KS, Smithies O** 1993 Alteration of reproductive function but not prenatal sexual development after insertional disruption of the mouse estrogen receptor gene. Proc Natl Acad Sci USA 90:11162–11166
39. **Smith EP, Boyd J, Frank GR, Takahashi H, Cohen RM, Specker B, Williams TC, Lubahn DB, Korach KS** 1994 Estrogen resistance caused by a mutation in the estrogen-receptor gene in a man. N Engl J Med 331:1056–1061
40. **Ekman P, Barrack ER, Greene GL, Jensen EV, Walsh PC** 1983 Estrogen receptors in human prostate: evidence for multiple binding sites. J Clin Endocrinol Metab 57:166–176
41. **Yager JD** 2000 Endogenous estrogens as carcinogens through metabolic activation. J Natl Cancer Inst Monogr 27:67–73
42. **Murphy JB, Emmott RC, Hicks LL, Walsh PC** 1980 Estrogen receptors in the human prostate, seminal vesicle, epididymis, testis, and genital skin: a marker for estrogen-responsive tissues? J Clin Endocrinol Metab 50:938–948
43. **Paech K, Webb P, Kuiper GG, Nilsson S, Gustafsson JA, Kushner PJ, Scanlan TS** 1997 Differential ligand activation of estrogen receptors ERα and ERβ at AP1 sites. Science 277:1508–1510
44. **Nojima D, Li LC, Dharia A, Perinchery G, Ribeiro-Filho L, Yen T-SB, Dahiya R** 2001 CpG hypermethylation of the promoter region inactivates the estrogen receptor-β gene in patients with prostate carcinoma. Cancer 92:2076–2083
45. **Chang WY, Prins GS** 1999 Estrogen receptor-β: implications for the prostate gland. Prostate 40:115–124
46. **Bonkhoff H, Stein U, Remberger K** 1991 The proliferative function of basal cells in the normal and hyperplastic human prostate. Prostate 24:114–118
47. **Weihua Z, Warner M, Gustafsson JA** 2002 Estrogen receptor beta in the prostate. Mol Cell Endocrinol 193:1–5

PERGAMON

European Journal of Cancer 39 (2003) 1552–1561

European Journal of Cancer

www.ejconline.com

EBAG9/RCAS1 expression in hepatocellular carcinoma: correlation with tumour dedifferentiation and proliferation

T. Aoki[a], S. Inoue[b], H. Imamura[a,*], J. Fukushima[d], S. Takahashi[c], T. Urano[b], K. Hasegawa[a], T. Ogushi[c], Y. Ouchi[b], M. Makuuchi[a]

[a]*Division of Hepato-Biliary-Pancreatic and Transplantation Surgery, Department of Surgery, University of Tokyo, 7-3-1 Hongo, Bunkyo-ku, Tokyo 113-8655, Japan*

[b]*Department of Geriatric Medicine, University of Tokyo, 7-3-1 Hongo, Bunkyo-ku, Tokyo 113-8655, Japan*

[c]*Department of Urology, Graduate School of Medicine, University of Tokyo, 7-3-1 Hongo, Bunkyo-ku, Tokyo 113-8655, Japan*

[d]*Department of Pathology, Teikyo University School of Medicine, 2-11-1 Kaga, Itabashi-ku, Tokyo 173-8606, Japan*

Received 5 December 2002; received in revised form 17 February 2003; accepted 3 April 2003

Abstract

The oestrogen-responsive gene, *EBAG9*, whose product is identical to the cancer cell surface antigen RCAS1, is reported to be associated with tumour progression and invasiveness in various carcinomas. In this study, we examined the expression of EBAG9/RCAS1 in hepatocellular carcinoma (HCC), with special reference to its relationship with the stepwise evolution of HCC. Expression was examined by immunohistochemistry and western blotting analysis in 143 HCCs, as well as in non-cancerous liver tissues. After which, the association between enhanced EBAG9/RCAS1 expression and various clinicopathological parameters including Ki-67 labelling index (LI), a marker of proliferative activity, was evaluated. There was a constant low level of EBAG9/RCAS1 expression in non-cancerous liver tissues, with a regular cytoplasmic distribution. Positive immunoreactivity for EBAG9/RCAS1 was detected on the surface and in the cytoplasm of 84 HCC tumours, with an irregular staining pattern. Enhanced EBAG9/RCAS1 expression was correlated with a lower degree of differentiation and Ki-67 LI. Interestingly, expression was enhanced specifically in the less differentiated lesions within 'nodule-in-nodule' tumours. In conclusion, EBAG9/RCAS1 was associated with HCC tumour dedifferentiation and increased proliferative activity. Its exact functional role remains to be established.

Keywords: EBAG9/RCAS1; Hepatocellular carcinoma; Immunohistochemistry; Western blotting analysis; Tumour dedifferentiation; Tumour proliferation; Ki-67 labelling index

1. Introduction

ER-binding fragment-associated antigen 9 (EBAG9) was originally identified as a human oestrogen-responsive gene in a cDNA library of MCF-7 human breast cancer cells, and its mRNA was shown to be directly upregulated by oestrogen [1]. By preparing a rabbit polyclonal antibody against EBAG9, we showed that it is upregulated by oestrogen *in vivo* in the mouse uterus, and that it is also expressed in various other mouse tissues, including the liver [2]. It has been reported recently, in a study using the same antibody, that EBAG9 is also widely distributed in human breast carcinomas [3].

Receptor-binding cancer antigen expressed on SiSo cells (RCAS1), which was isolated as the antigen recognised by 22-1-1 antibody against a human uterine adenocarcinoma cell line SiSo [4], has been shown to be identical to EBAG9 (EBAG9/RCAS1) [5]. It has received attention as a potential cancer-associated antigen in various organs [4,6–16]. Expression is generally thought to be related to tumour invasiveness and also to be associated with a poor patient prognosis. It has been suggested that the close relationship between EBAG9/RCAS1 expression and tumour invasiveness may be accounted for by the *in vitro* observation that this protein facilitates escape from host immune surveillance by inducing apoptosis of activated $CD3^+$ T lymphocytes and NK cells [5].

Hepatocellular carcinoma (HCC) has the unique characteristic that its development and progression

* Corresponding author. Tel.: +81-3-3815-5411x33321; fax: +81-3-5684-3989.

E-mail address: himamura-tky@umin.ac.jp (H. Imamura).

0959-8049/03/$ - see front matter © 2003 Elsevier Ltd. All rights reserved.
doi:10.1016/S0959-8049(03)00362-9

exhibits a typical multistep pathology [17]. In general, most early HCCs [18,19] are small (< 2 cm in diameter), well-differentiated nodules with a low proliferative activity, and their size remains unchanged for months or, in some cases, years. When they progress to a more advanced stage, they transform into moderately- to poorly-differentiated cancers, accompanied by a rapid increase in size. During this process (tumour dedifferentiation and proliferation), the HCCs also increase in malignant potential, as reflected in intrahepatic metastasis (IM) and vascular invasion (VI). This transformation occurs non-uniformly within a given tumour nodule, resulting in the coexistence of well-differentiated and moderately- to poorly-differentiated lesions within the same nodule. This has been termed by histologists a 'nodule-in-nodule' or 'mosaic' appearance [17].

It was previously reported that RCAS1 expression could not be detected in normal liver samples probed with 22-1-1 antibody, but was found in approximately one quarter of HCC cases, particularly in patients with VI of the tumour [16]. Expression of EBAG9/RCAS1 has, however, not yet been investigated in detail in relation to the multistep progression of HCC. In the present study, we have investigated the association of its expression with the successive stages of HCC progression by immunohistochemistry and western blot analysis utilising a rabbit anti-EBAG9 polyclonal antibody. We paid particular attention to (1) the process of tumour dedifferentiation, (2) cancer proliferative activity, and (3) ability to metastasise. We evaluated cancer proliferative activity by the Ki-67 labelling index (LI), which has been used as a marker of proliferation in various cancers including HCC [20,21]. We also examined the correlation between EBAG9/RCAS1 immunoreactivity and various clinical parameters, including disease-free survival.

2. Patients and methods

2.1. Study population and follow-up of patients

From October 1994 to December 1998, 232 radical hepatic resections were performed for HCC in the Hepato-Biliary-Pancreatic and Transplantation Division, Department of Surgery, Tokyo University Hospital, Tokyo. Among them, 58 of the patients received repeat hepatectomies for recurrent tumours, and 6 underwent hepatic resection for mixed HCC and cholangiocarcinoma [22], and these cases were excluded from the study population. In addition, 25 patients were excluded because of totally necrotised tumours caused by preoperative transcatheter arterial embolisation or chemo-lipiodolisation. The 143 patients enrolled included 109 males and 34 females, with a mean age of 62.0±11.0 (mean±standard deviation (S.D.)) years (range 13–83 years). 23 patients were positive for hepatitis B surface antigen (HBs Ag), and 100 for anti-hepatitis C virus antibody (HCV Ab). One patient was positive for both.

At hepatectomy, resected liver specimens were fixed in 10% v/v formalin, cut into blocks, and embedded in paraffin. They were then sliced into 4-μm sections, and stained with haematoxylin and eosin, or used for immunohistochemical analysis. A part of each tumour, as well as adjacent non-cancerous tissue, was snap frozen in liquid nitrogen and stored at −80 °C for later protein isolation.

Normal liver tissue was obtained for the immunohistochemical analysis from 10 potential liver transplant donors, who provided liver biopsy specimens for preoperative evaluation. Ten liver biopsies carried out for the assessment of serologically HCV Ab positive patients were also made available for analysis.

Follow-up data were obtained from medical records or telephone interviews and were available in 142 cases. They were updated for patient's disease-free survival to 30 June 2002 (mean follow-up period 45.5 months, range 6.3–85.8 months). The patients received monthly abdominal ultrasonography and their levels of alpha-fetoprotein (AFP) (normal range < 20 ng/ml) and des-γ-carboxy prothrombin (DCP) (normal range < 62.5 AU/ml) were measured. In addition, they underwent dynamic computed tomography (CT) at least every 6 months. Angiography with lipiodol injection was added when recurrence was suspected and recurrence was assessed by a combination of these imaging modalities.

2.2. Serology

EBAG9 antibody was a rabbit polyclonal antibody against a glutathione-S-transferase (GST)-EBAG9 fusion protein [2]. Its specificity has been examined previously in Ref. [3]; in summary, it was shown to react with human and mouse EBAG9, yielding a band of 32kD in western blotting analysis, and the intensity of the band was reduced by prior incubation of the antibody with recombinant EBAG9 protein. Monoclonal antibody for Ki-67 (MIB 1) and monoclonal antibody for β-actin (Clone AC-74) were purchased from DAKO (Carpinteria, CA, USA) and Sigma-Aldrich (Saint Louis, MI, USA), respectively.

2.3. Immunohistochemistry

Tissue sections of each HCC nodule and adjacent non-cancerous liver tissue, as well as the liver biopsy specimens, were submitted to immunohistochemical analysis. Where there were multiple nodules the largest nodule was considered to be representative. After removing paraffin in xylene, and rehydrating in a graded ethanol series, the sections were processed in 10 mM

citrate buffer (pH 6.0) and heated in an autoclave at 125 °C for 5 min for antigen retrieval. Endogenous peroxidase activity was quenched with 3% v/v hydrogen peroxidase/methanol. The slides were preincubated with 10% v/v fetal calf serum-phosphate buffered saline at room temperature to reduce non-specific antibody binding. They were then incubated overnight at 4 °C with the EBAG9 antibody diluted 1:40, or with the Ki-67 antibody diluted 1:50. Immunostaining was performed by a peroxidase labelled-dextran polymer method using EnVision + TM (DAKO, Carpinteria, CA, USA). Staining was visualised with 3,3′-diaminobenzidine tetrahydrochloride working solution (Funakoshi, Tokyo, Japan), with counterstaining in Mayer's haematoxylin. For negative controls, primary antibody was replaced with normal rabbit (diluted 1:800) or mouse (diluted 1:100) IgG (DAKO, Carpinteria, CA, USA). Sections of human breast cancer that had been shown to be EBAG9-positive were processed as positive controls.

Scoring of Ki-67 in HCCs was performed on high-power fields (×400) by light microscopy. In each case, more than 500 carcinoma cell nuclei were counted independently by two of the authors, and the percentage of immunoreactive cells, that is, LI, was determined. Final scores were established by consensus.

2.4. Western blotting analysis

Western blotting was performed on representative samples of HCC and non-cancerous liver tissue. Frozen sections of five HCC tissues and adjacent non-cancerous liver tissues (all histologically diagnosed as cirrhotic) were homogenised on ice in RIPA buffer (50 mM Tris–HCl (pH 8.0), 200 mM NaCl, 20 mM NaF, 2 mM ethyleneglycol tetraacetic acid, 1 mM dithiothreitol, 2 mM sodium vanadate, 0.5% v/v Nonidet P-40 supplemented with protease inhibitor cocktail (Complete™; Boehringer Mannheim GmbH, Mannheim, Germany)). The homogenates were clarified by centrifugation at 12 000*g* for 30 min at 4 °C. Samples of lysates containing 8 μg protein [23] were boiled for 5 min in the presence of β-mercaptoethanol. They were then fractionated on 10–20% w/v sodium dodecyl sulphate (SDS)-polyacrylamide gradient gel and transferred electrophoretically onto a polyvinylidene difluoride membrane (Fluorotrans, Japan Genetics, Tokyo, Japan) using a buffer consisting of 25 mM Tris, 192 mM glycine, and 20% v/v methanol. The membrane was blocked at room temperature for 30 min in Tris-buffered saline with 1% v/v Tween 20 (TBS-T) and 5% w/v skimmed milk, then incubated overnight at 4 °C with rabbit anti-EBAG9 serum diluted 1:1000 or mouse monoclonal antibody against β-actin diluted 1:2500. The membrane was washed in TBS-T, and incubated with 1:5000 diluted horseradish peroxidase-conjugated donkey anti-rabbit IgG (Amersham Pharmatica Biotech, Tokyo, Japan) at room temperature for 1 h. After further washings, the protein–antibody complexes were visualised with the enhanced chemiluminescence (ECL™) plus detection system (Amersham Pharmatica Biotech, Tokyo, Japan) according to the manufacturer's protocol. A whole cell lysate of a human prostate cancer cell line, DU145, was used as a positive control.

2.5. Analysis of the association between EBAG9 expression and clinicopathological variables

The correlation between EBAG9 expression and various clinical and pathological parameters was analysed using the Chi-square or Mann–Whitney U test, as appropriate. Seven clinical and seven pathological variables were examined as follows: patient age (65 years versus ⩾65 years), gender, HBs Ag, HCV Ab, Child–Turcotte–Pugh score (Grade A versus B) [24], serum AFP level, plasma DCP level, degree of tumour differentiation (well versus moderately or poorly), size of largest tumour nodule (⩽2.0 versus >2.0), tumour number (solitary versus multifocal), microscopic IM and/or microscopic VI, fibrous capsular formation/infiltration, pathology of non-cancerous liver tissue (fibrosis versus chronic hepatitis versus cirrhosis) and Ki-67 LI. The presence of microscopic IM and/or microscopic VI was clustered into a single variable and defined as tumour invasiveness [25]. When a tumour nodule contained components of different grades of differentiation, the tumour was classified according to the predominant grade. A P value of 0.05 was considered statistically significant.

To detect factors associated with patient's disease-free survival, univariate analysis was performed using Cox proportional hazards model for EBAG9 or other clinicopathological variables, and the risk ratio and 95% Confidence Intervals (CI) were calculated [26]. Data were analysed using the StatView 5.0J software (SAS Institute Inc., Cary, NC, USA).

3. Results

3.1. EBAG9 expression in normal and chronically diseased liver tissue

Non-cancerous hepatocytes, including those from normal, chronic HCV-related hepatitic or cirrhotic tissues, displayed a low, but significant, level of EBAG9 immunoreactivity compared with negative controls (Fig. 1a–e). High power magnification (×1000) revealed punctate staining throughout the cytoplasm (Fig. 1c).

3.2. EBAG9 expression in HCCs

HCC cells showed variable EBAG9 immunoreactivity. Some had baseline weak immunoreactivity

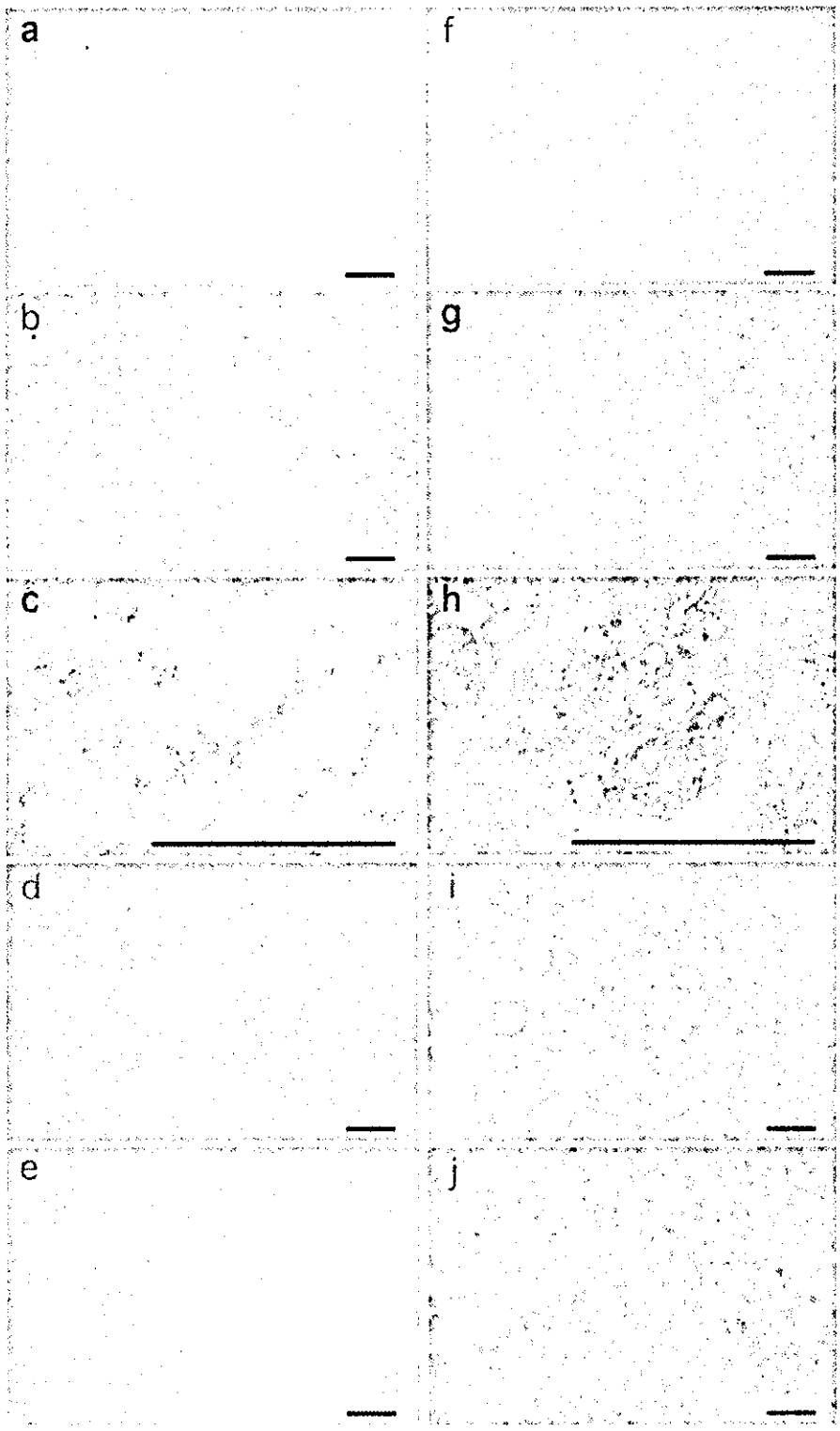

Fig. 1. Expression of ER-binding fragment-associated antigen 9 (EBAG9) in non-cancerous liver tissues (a–e) and hepatocellular carcinomas (HCCs) (f–j). (a) Negative controls showing no immunoreactivity (×200). (b–e) Normal liver tissue (b), chronic hepatitic tissue (d), and cirrhotic tissue (e) showing weak immunoreactivity (×200). A regular distribution of weakly stained dots is seen in the cytoplasm of normal hepatocytes (c) (×1000). (f) A well-differentiated HCC classified as intensity-negative. The pattern of expression is similar to that in non-cancerous tissues (×200). (g and h) An intensity-positive case of moderately-differentiated HCC (trabecular type) (g) (×200). Immunoreactivity is detected over the entire surface and in the cytoplasm of the cancer cells. Coarse, thickened granules are dispersed in the cytoplasm, and the regularity of the staining pattern is lost (h) (×1000). (i) Pseudoglandular type of moderately-differentiated HCC displaying intense expression on the apical surface of the cells (×200). (j) A poorly-differentiated HCC consisting of small cells with enhanced EBAG9 expression on their surface and in the cytoplasm (×200). Bar: 20 μm.

similar to non-cancerous hepatocytes. These were designated intensity-negative cells. Others showed enhanced immunoreactivity, and were designated intensity-positive. With regard to staining pattern, intensity-negative cancer cells had a similar pattern to non-cancerous hepatocytes, namely, a regular distribution of weakly stained granules throughout the cytoplasm (Fig. 1f). In contrast, in most of the intensity-positive cells, there was intense staining over the entire surface, as well as in the cytoplasm (Fig. 1g-j). Coarse, thickened granules were dispersed throughout the cytoplasm, and the regularity of the granule distribution noted in the non-cancerous hepatocytes was lost (Fig. 1h). In the pseudoglandular type of moderately differentiated HCCs, the apical surfaces of the pseudoglands were strongly stained (Fig. 1i).

The proportion and distribution of intensity-positive cancer cells were highly variable from nodule to nodule (range 5–100%). Interestingly, their distribution also showed two types of intranodular diversity: (1) 'Nodule-in-nodule' tumours, i.e. those consisting of a well-differentiated lesion and a less differentiated lesion, displayed different immunoreactivity in the two regions, the less differentiated intensely immunoreactive region contrasting clearly with the weakly immunoreactive well-differentiated region (Fig. 2a). (2) The peripheral zone of HCC nodules with fibrous capsular infiltration stained strongly at the site of infiltration (Fig. 2b).

3.3. Semiquantitative classification of EBAG9 expression in HCCs

We next evaluated the expression of EBAG9 in HCC tissues in a semiquantitative manner. We classified sections into three categories: (1) Negative (−): sections in which all the cancerous cells were identified as intensity-negative; (2) borderline (±): sections where 1–5% of the malignant cells stained for EBAG9, or, sections showing uniform positivity but very weak immunoreactivity; (3) positive (+): sections with more than 5% of positive cancerous cells. The classification of the sections was carried out in a blinded manner and finally agreed upon by two of the authors. In the event, 35 of the 143 lesions examined (24%) were classified as negative, 24 (17%) as borderline, and 84 (59%) as positive (Table 1).

3.4. Western blotting analysis

The results of the western blotting analysis are shown in Fig. 3. All the non-cancerous tissues expressed EBAG9 as a 32-kD band. Expression of EBAG9 was not enhanced in two of the five cancerous tissues examined (cases 1 and 2: one well-differentiated and one moderately-differentiated HCC); however, it was enhanced in the remaining three samples (cases 3–5: moderately-differentiated HCCs). The division of HCCs by western blotting analysis into those in which expression of EBAG9 was enhanced, and those in which it was not, agreed well with the classification into intensity-positive/-negative nodules by semiquantitative immunohistochemistry.

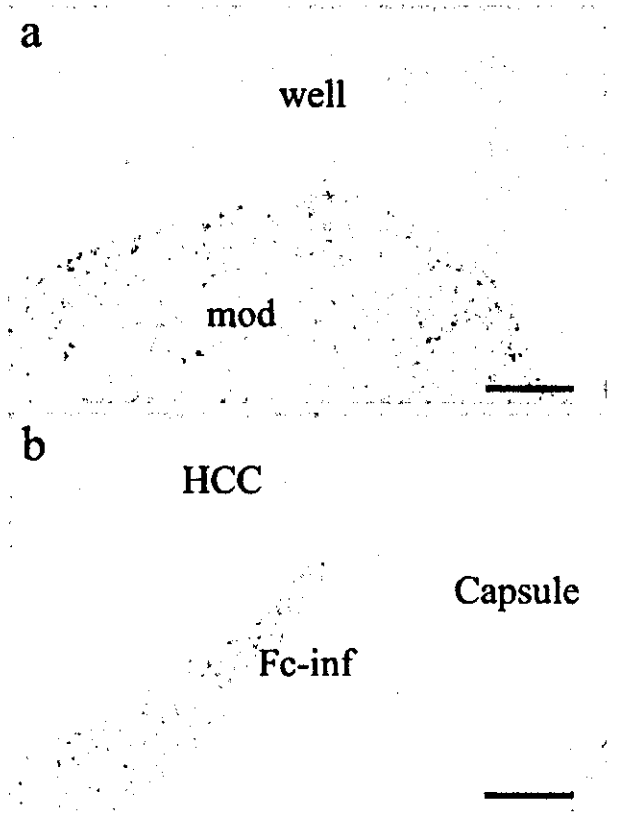

Fig. 2. Distribution of intensity-positive cancer cells in hepatocellular carcinomas (HCC) nodules: (a) a tumour with 'nodule-in-nodule' appearance showing intense staining in the interior moderately-differentiated region ('mod'), contrasting with weak staining in the outer, well-differentiated, region ('well') (×100); (b) a moderately-differentiated HCC showing fibrous capsular infiltration ('Fc-inf') with enhanced staining at the site of infiltration (×100). Capsule: fibrous capsule. Bar: 50 μm.

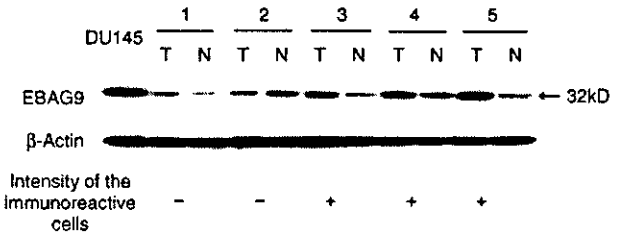

Fig. 3. Western blotting analysis. All non-cancerous liver samples (N) express ER-binding fragment-associated antigen 9 (EBAG9) as a 32-kD band. Expression of EBAG9 is not enhanced in two of the hepatocellular carcinomas (HCCs) (1 and 2), but is enhanced in the other 3 (3–5). The results of the western blotting analysis are consistent with the classification based on the immunohistochemistry. Western blotting using monoclonal anti-β-actin antibody demonstrated that equal amounts of protein were used. T, HCC tissue; N, non-cancerous liver tissue; kD, kilodalton.

Table 1
Frequency distribution of immunocytochemical staining of HCCs for EBAG9

Classification of staining	Notation	Number of HCC tumours	Percentage of HCC tumours
Negative	–	35	24
Borderline	±	24	17
Positive	+	84	59
Total		143	100

HCC, Hepatocellular carcinoma; EBAG9, ER-binding fragment-associated antigen 9.

3.5. Correlation between EBAG9 expression and pathological variables

For the purpose of analysis, unless otherwise specified, the borderline staining HCCs were combined with the unstained tumours into one group, leaving the clearly positive staining HCCs as the other group. The relationship between EBAG9 immunoreactivity and clinicopathological variables was then analysed by comparing the intensity-positive group ($n=84$) with the intensity-negative/borderline group ($n=59$), as shown in Table 2. Enhanced EBAG9 immunoreactivity was more frequently observed in the less differentiated tumours ($P=0.01$). In addition, EBAG9 immunoreactivity was significantly related to Ki-67 LI (Fig. 4). In the intensity-negative/borderline group, the mean Ki-67 LI was 16.4% (median 12.6, range 0.5–56.0) whereas it was 24.8% in the intensity-positive group (median 23.8, range 2.9–68.6) ($P<0.001$). However, there was no significant correlation between enhanced EBAG9 expression and tumour invasiveness (IM and/or VI) ($P=0.86$). Other clinical and pathological variables were also not significantly associated with enhanced EBAG9 expression, although the relationship between enhanced EBAG9 expression and elevated plasma DCP value was of borderline significance ($P=0.1$).

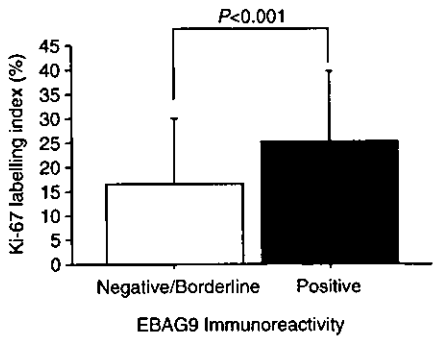

Fig. 4. Association of ER-binding fragment-associated antigen 9 (EBAG9) expression with Ki-67 labelling index (LI).

3.6. Relationship between EBAG9 expression and disease-free survival

During the follow-up period, HCC recurrence was confirmed in 107 patients. On the univariate analysis, plasma DCP level, tumour size, tumour number, tumour invasiveness (IM and/or VI), and Ki-67 LI (>20 versus ≤ 20) were significantly related to the patient's disease-free survival (Table 3). However no significant relationship was established between enhanced EBAG9 expression and disease-free survival ($P=0.17$).

4. Discussion

In the present study, we have investigated the expression of EBAG9/RCAS1 in various HCC and non-HCC liver tissues, including those from normal livers and those chronically infected with HCV and/or HBV. We performed a comprehensive immunohistochemical analysis using a specific antibody against EBAG9 which is also suitable for western blotting analysis, paying special attention to the association of EBAG9 expression with tumour dedifferentiation, proliferation and metastasis.

EBAG9/RCAS1 was expressed, albeit weakly, in both normal and chronically diseased non-cancerous hepatocytes. In addition, it showed a regular pattern of expression within the cytoplasm, suggesting that it becomes localised in some way. The finding of EBAG9/RCAS1 in non-cancerous hepatocytes contradicts the results of a previous report [16]. However, it is consistent with the detection of EBAG9/RCAS1 expression in a number of non-cancerous human organs, e.g., uterine endometrial glands [27], goblet cells of bronchi and bronchioles [7,8], mammary glands [3], and gastric mucosa [10]. It is notable that the apical surfaces of the pseudoglands were strongly stained in the pseudoglandular type of moderately-differentiated HCCs, as shown in Fig. 1i. This observation, together with previous results obtained from normal tissues, suggests that EBAG9/RCAS1 is expressed in gland cells.

In this study, 59 and 17% of the patients examined showed positive and borderline expression of EBAG9/RCAS1, respectively. This roughly agrees with the proportion found in other malignancies (47% in lung cancers to 70% in gallbladder cancers) [8,11]. However, Noguchi and colleagues reported that only 26.5% of HCC cases expressed RCAS1 compared with the 59% showing positivity for EBAG9 reported above [16]. We can be confident that our immunohistochemical staining for EBAG9 is specific for this protein for the following reasons: (a) The specificity of the anti-EBAG9 polyclonal antibody has been established by the preabsorption test reported previously in Ref. [3]. (b) In western

Table 2
Association between EBAG9 immunoreactivity and clinicopathological parameters

Parameters	Number of patients	Intensity of EBAG9 immunoreactivity		*P* value
		Negative/borderline (%)	Positive (%)	
		62.2±11.6	61.8±10.6	0.44
Age (years)[a]				
<65	75	28 (37)	47 (62.7)	
⩾65	68	31 (46)	37 (54.4)	0.39
Gender				
Male	107	40 (37)	67 (62.6)	
Female	36	19 (53)	17 (47.2)	0.12
HBs Ag				
+	23	10 (43)	13 (56.5)	
−	120	49 (41)	71 (59.2)	0.82
HCV Ab				
+	100	42 (42)	58 (58.0)	
−	43	17 (40)	26 (60.5)	0.85
Child–Turcotte–Pugh score				
A	110	43 (39)	67 (60.9)	
B	33	16 (48)	17 (51.5)	0.42
AFP (ng/ml)[b]		51 (2–436 000)	55 (2–69 000)	0.57
⩽62.5	48	17 (35)	31 (65)	
>20	95	42 (44)	53 (56)	0.37
DCP (AU/ml)[b]		62.5 (11–80 000)	76.0 (10–77 520)	0.10
⩽6.25	76	36 (47)	40 (53)	
>62.5	67	23 (34)	44 (66)	0.12
Degree of tumour differentiation				
Well	25	16 (64)	9 (36)	
Moderately/poorly	118	43 (36)	75 (64)	0.01
Tumour size (cm)[a]		2.8 (0.8–15.5)	3.4 (1.0–16.0)	0.29
⩽2.0	38	20 (53)	18 (47)	
>2.0	105	39 (37)	66 (63)	0.12
Tumour number				
Solitary	79	35 (44)	44 (56)	
Multifocal	64	24 (38)	40 (63)	0.49
IM and/or VI				
Positive	58	23 (40)	35 (60)	
Negative	85	36 (42)	49 (58)	0.86
Fibrous capsular formation/infiltration				
Positive/positive	79	30 (38)	49 (62)	
Positive/negative	27	13 (48)	14 (52)	
Negative	37	16 (43)	21 (57)	0.62
Background liver disease				
Liver fibrosis	5	1 (20)	4 (80)	
Chronic hepatitis	40	13 (33)	27 (68)	
Liver cirrhosis	98	45 (46)	53 (54)	0.21
	143	59 (46)	84 (59)	

EBAG9; ER-binding fragment-associated antigen 9; HBs Ag, HBs Ag-positive; HCV Ab, HCV Ab-positive; AFP, alpha-fetoprotein; DCP, des-β-carboxy prothrombin; IM, intrahepatic metastasis; VI, vascular invasion.

[a] Data expressed as average±standard deviation (S.D.).

[b] Data expressed as median value (range).

blots, the EBAG9 antibody recognised a protein forming a specific 32-kD band, consistent with the size of human EBAG9. (c) The intensity of the 32-kD band agreed with the semiquantitative classification of EBAG9 immunoreactivity by immunohistochemistry. Therefore, the fact that the proportion of EBAG9-positive patients was almost as twice as high in our series is not the result of non-specific staining. It may be due to the different antibodies and methods used in the two studies.